

# Ecological Effects of Artificial Mixing in Lake Rotoehu



**May 2015**

## **ERI Report 59**

Client report prepared for Bay of Plenty Regional Council

By Chris G. McBride<sup>1</sup>, Grant W. Tempero<sup>1</sup>, David P. Hamilton<sup>1</sup>, Brian T. Cutting<sup>1</sup>, Kohji Muraoka<sup>1</sup>, Ian C. Duggan<sup>1</sup> and Max M. Gibbs<sup>2</sup>

<sup>1</sup>Environmental Research Institute  
Faculty of Science and Engineering  
University of Waikato, Private Bag 3105  
Hamilton 3240, New Zealand

<sup>2</sup>NIWA Hamilton  
Gate 10 Silverdale Road  
Hillcrest, Hamilton 3216

**Cite report as:**

McBride CG, Tempero GW, Hamilton DP, Cutting BT, Muraoka K, Duggan IC and Gibbs M 2015. Ecological Effects of Artificial Mixing in Lake Rotoehu. *Environmental Research Institute Report No. 59*. The University of Waikato, Hamilton. 70 pp.

**Disclaimer:**

The information and opinions provided in the Report have been prepared for the Client and its specified purposes. Accordingly, any person other than the Client, uses the information and opinions in this report entirely at their own risk. The Report has been provided in good faith and on the basis that reasonable endeavours have been made to be accurate and not misleading and to exercise reasonable care, skill and judgment in providing such information and opinions.

Neither The University of Waikato, nor any of its employees, officers, contractors, agents or other persons acting on its behalf or under its control accepts any responsibility or liability to third parties in respect of any information or opinions provided in this Report.

*Reviewed by:*



Moritz Lehmann

University of Waikato

Research Fellow

*Approved for release by:*



John Tyrell

University of Waikato

Research Manager

## Executive summary

Lake Rotoehu is a eutrophic, moderately large (795 ha), shallow (mean depth 8.2 m), polymictic lake in the Rotorua/Te Arawa lake district. Land use intensification, water level changes, and nutrient-rich geothermal inflows are some of the factors which may have contributed to severe cyanobacteria blooms over the past 20 years.

Bay of Plenty Regional Council (BoPRC) is charged with maintaining the ecosystem health of Lake Rotoehu. In 2007 BoPRC published the Lake Rotoehu Action Plan, outlining multiple restoration initiatives to reduce nutrient loading to the lake. Among these initiatives was a trial of artificial mixing to increase vertical circulation within the water column, preventing the formation of stratification. Two water column mixing devices were deployed on the lake bed of Lake Rotoehu from November 2012 to June 2014 (and are ongoing). These devices force compressed air through a diffuser near the bottom of the lake water column in the central lake basin. Buoyancy caused by the rising bubbles draws water from the bottom of the lake up through large vertical cylinders to the surface, where the entrained water is subsequently directed horizontally along the water surface. The University of Waikato was contracted to monitor the physical (temperature and dissolved oxygen), chemical (nutrients), and biological (phytoplankton and zooplankton) effects of the mixing devices on the lake. This work encompassed a range of instrumentation, laboratory analyses, and species enumeration from water samples.

In addition, an evaluation of the area of effect and strength of current generated by the mixing devices was conducted by the National Institute of Water and Atmospheric Research (NIWA), the results of which are reported here. Rhodamine dye tracer injected into the northern arm of the southern mixing device revealed that cooler hypolimnetic water was being brought to the surface. A component of the water entrained in this plume flowed away from the mixing device for at least 90 m. Parts of the plume also detrained from it, sinking towards the thermocline. Plumes from the mixing devices were tracked by Acoustic Doppler Current Meters (ADCM) or Profilers. The ADCM data revealed that the plume gradually dispersed laterally with increasing distance from the mixing device, and plume velocities were not elevated above background levels at c. 70 m from the mixing device. Although current velocities measured in the plume were generally low ( $<1 \text{ cm s}^{-1}$  to  $25 \text{ cm s}^{-1}$ ; average  $5.5 \text{ cm s}^{-1}$ ) they could be clearly distinguished from wind driven currents.

Changes to the water column thermal profile were observed adjacent to the mixing devices, however, modification of the water column temperature structure across the lake (i.e., greater than a hundred metres from the devices) was not observed. Interpretations of the effect of the aeration devices was somewhat confounded by the

period prior to installation of the machines (summer 2012) being cold and windy relative to weather conditions during the period of device deployment, which were unusually hot and dry (summer 2013 and 2014). These conditions resulted in Lake Rotoehu being stratified more often and strongly than in the summer prior to device installation. Additional factors affecting the aeration device operation are discussed in the report.

Analyses of nutrient concentrations, water clarity, and trophic status indicators have shown some improvement of Lake Rotoehu over recent years. However, the Trophic Level Index (TLI) has not yet met the target of 3.9 specified by the Rotoehu Action Plan. Water quality assessed by these indicators was comparatively good in 2012 – June 2014 despite the sustained periods of thermal stratification that contributed to significant oxygen depletion in bottom waters.

Localised effects of mixing included homogenisation of the cyanobacterial community through the water column and a decrease in the Bray-Curtis similarity index of the plankton community between mixing sites (i.e. near the aeration device) and controls (i.e. several hundred metres away from the mixing device). These results are consistent with physical observations of localised changes in thermal structure around the aeration devices. No significant changes occurred in plankton community composition at the whole-lake scale during aerator operation during the 2013 and 2014. By contrast, plankton community composition showed large seasonal and inter-annual variability including presence of invasive species.

Results suggest that the mixing devices installed in Lake Rotoehu are able to draw hypolimnetic water to the surface. The resulting horizontal plume rapidly becomes mixed with surface waters over distances of 50–60 m from the aerator but can also be tracked as it plunges towards the thermocline at these distances. Some localised effects were detected near the aerators but there were no detectable lake-scale effects. By contrast, there have been progressive improvements in water quality at a whole-lake scale over recent years and these may relate to alum dosing of the major geothermal inflow to the lake, weed harvesting and initial decreases in external nutrient inputs in response to changes in land use and land-use practices. Further monitoring will help clarify these observations, and an additional year of mixing device deployment aims to improve operational efficiency of the devices and quantify effects of proposed increases in air flow rates.

## Acknowledgements

We acknowledge the valuable contributions of Andy Bruere, John McIntosh, Paul Scholes and the staff of BoPRC. Field assistance was ably provided by Joseph Butterworth, Warrick Powrie and Josh de Villiers. We thank Sarah Cross and Eloise Brown for identification and enumeration of phytoplankton data. Jeremy Garrett-Walker is gratefully acknowledged for his assistance with the analysis of community data. We also acknowledge the advice and guidance from Deniz Özkundakci. Moritz Lehmann and John Tyrrell are thanked for reviewing this report. Funding of this project was provided by BoPRC and included support of the Bay of Plenty Chair in Lake Restoration the University of Waikato. Additional support was through the Outcome Based Investment in Lake Biodiversity Restoration, funded by the Ministry of Business, Innovation and Employment (contract UOWX0505).

## Table of contents

<b>Executive summary .....</b>	<b>iii</b>
<b>Acknowledgements.....</b>	<b>v</b>
<b>Table of contents .....</b>	<b>vi</b>
<b>List of figures.....</b>	<b>vii</b>
<b>List of tables.....</b>	<b>xi</b>
<b>Introduction .....</b>	<b>12</b>
Threats to lake systems.....	12
Lake Rotoehu.....	12
Artificial destratification.....	13
<b>Methods .....</b>	<b>16</b>
Site description.....	16
Meteorology.....	17
Monitoring buoy – fixed sensors.....	17
Monitoring buoy – Water column profiling sensors.....	17
CTD Profiles .....	17
Bio-Fish .....	18
Chlorophyll, nutrients and Secchi disk depth .....	18
Dye tracer study .....	18
Current measurements .....	19
Plankton community sampling.....	19
Mixing device operation.....	20
<b>Results .....</b>	<b>22</b>
Monitoring buoy – fixed sensors.....	22

Profiler Buoy.....	23
Meteorological data .....	25
CTD and Bio-fish profiles .....	26
Dye tracer study .....	35
Current measurements .....	36
Nutrient and chlorophyll concentrations.....	40
Plankton communities .....	46
<b>Discussion .....</b>	<b>57</b>
<b>Conclusions .....</b>	<b>61</b>
<b>References .....</b>	<b>63</b>
<b>Appendix 1.....</b>	<b>66</b>

## List of figures

<b>Figure 1.</b> Historical Trophic Level Index (TLI) of Lake Rotoehu from 1991 to 2013 (BoPRC). .....	13
<b>Figure 2.</b> Map of Lake Rotoehu showing sampling locations. Destratification devices are represented by orange triangles. Blue circles represent sampling locations. The profiler buoy is also located at sampling Site 1. The green cross marks the location of the primary (central lake) BoPRC monitoring site. The fixed sensor monitoring buoy location is represented by the red square and profiling buoy location with a green square. The purple dashed line indicates the route taken (south to north) during Bio-Fish surveys which ended at Site F. ....	16
<b>Figure 3.</b> Illustration of Bio-Fish set-up. The size of the boat has been scaled down approximately 10-fold compared with the Bio-Fish device and on-board installation. 18	
<b>Figure 4.</b> Installation of the mixing devices in Lake Rotoehu. Images by A. Bruere. ....	21
<b>Figure 5.</b> Temperature of air and water at different depths based on records from the Lake Rotoehu monitoring buoy for the period April 2011 to December 2014.....	22
<b>Figure 6.</b> Percent saturation of dissolved oxygen at two depths, based on records from the Lake Rotoehu monitoring buoy for the period April 2011 to December 2014. Sections of data have been corrected for electronic sensor drift.....	22

<b>Figure 7.</b> Schmidt stability index of Lake Rotoehu, based on records from the Lake Rotoehu monitoring buoy for the period April 2011 to December 2014. A higher Schmidt stability value indicates stronger stratification of the water column. ....	23
<b>Figure 8.</b> Water temperature at different depths in Lake Rotoehu as measured by the profiler buoy between September 2013 and December 2014. Areas of grey represent insufficient resolution to allow interpolation of temperature. ....	23
<b>Figure 9.</b> Dissolved oxygen concentration at different depths in Lake Rotoehu as measured by the profiler buoy between September 2013 and December 2014. Areas of grey represent insufficient resolution to allow interpolation of dissolved oxygen. ....	24
<b>Figure 10.</b> Meteorological data from January 2009 to January 2015, including short wave radiation (SW), air temperature, vapour pressure, wind speed, atmospheric pressure and rainfall. Data were obtained from the Rotorua Airport climate station via the cliflo database (cliflo.niwa.co.nz, station number 1770) with daily means calculated from hourly measurements. ....	25
<b>Figure 11.</b> Comparison of CTD casts taken at Site 1 (mixing site) and Site 2 (control site) (c. 400 m from mixing device). Casts presented are prior to installation of the mixing devices. ....	27
<b>Figure 12.</b> Comparison of CTD casts taken at Site 1 (mixing site) and Site 2 (control site)(c. 400 m from mixing devices). The mixing devices were active from mid-November 2012. ....	28
<b>Figure 13.</b> Comparison of CTD casts taken at Site 1 (mixing site) and Site 2 (control site) (c. 400 m from mixing devices). The mixing devices were not in operation on 15 March, 28 June, 26 September and 24 October 2013. ....	29
<b>Figure 14.</b> Comparison of CTD casts taken at Site 1 (mixing site) and Site 2 (control site)(c. 400 m from mixing device). Mixing devices were in operation from 14 November 2013 to 13 June 2014. ....	30
<b>Figure 15.</b> Cross-section of Lake Rotoehu showing the undulating path of the Bio-Fish device from south (left) to north (right) through the water on 9 October 2012 for A) water temperature, B) dissolved oxygen concentration, and C) chlorophyll fluorescence. Fluorescence data are reduced near the water surface, likely indicating non-photochemical quenching (bright-light inhibition of phytoplankton fluorescence response). Orange arrows denote the location of the mixing devices. The Bio-Fish passed within 100 m of the southern machine, and approximately 350 m from the northern machine (see Figure 2). ....	31
<b>Figure 16.</b> Cross-section of Lake Rotoehu showing the undulating path of the Bio-Fish device from south (left) to north (right) through the water on 17 January 2013 for A) water temperature, B) dissolved oxygen concentration, and C) chlorophyll fluorescence. Orange arrows denote the location of the mixing devices. The Bio-Fish passed within 100 m of the southern machine, and approximately 350 m from the northern machine (see Figure 2). ....	32



- Figure 17.** Cross section of Lake Rotoehu showing the undulating path of the Bio-Fish device from south (left) to north (right) through the water on 22 February 2013 for A) water temperature, B) dissolved oxygen concentration, and C) chlorophyll fluorescence. The lake was strongly stratified with evidence of oxygen depletion in bottom waters. Note uneven depth of stratification across the transect. Orange arrows denote the location of the mixing devices. The Bio-Fish passed within 100 m of the southern machine, and approximately 350 m from the northern machine (see Figure 2). .....33
- Figure 18.** Cross-section of Lake Rotoehu showing the undulating path of the Bio-Fish device from south (left) to north (right) through the water on 01 March 2013 for A) water temperature, B) dissolved oxygen concentration and C) chlorophyll fluorescence. Orange arrows denote the location of the mixing devices. The Bio-Fish passed within 100 m of the southern machine, and approximately 350 m of the northern machine (see Figure 2). The mixing devices were turned off on this occasion, although the lake was already fully mixed on this day.....34
- Figure 19.** Dye plume produced on the lake surface. Mixing device and dye metering equipment on the left with a surface plume visible moving towards the right (north). .....35
- Figure 20.** Contour plot of the dye plume from the mixing device on 27 February 2013 using Surfer32 by Golden Software. Vertical lines are profiling points. Interpolation between points used triangulation with a ratio of 12:1. The contour plot is a representation of the likely dye flow path based on the available data. ....35
- Figure 21.** Boat path (continuous circular line) of the bottom-tracking ADCP used to locate and define the current flow from each of the arms of the mixing device. The overlay is a stylised representation of the current plume dispersion patterns arbitrarily labelled A, B and C. The Rhodamine dye was injected into arm C.....36
- Figure 22.** Example of the flow pattern from the southern mixing device through the water column depth adjacent to the western arm of the device (Figure 22, arm A) at a distance of 12 m as raw data. The colours represent the 4 acoustic profiler beams. The horizontal axis is “instrument intensity” as counts. The counts are relative to the background intensity slope. ....37
- Figure 23.** Progressive 'drifter' plots of A) wind and water movement at B) 3 m depth, C) 6 m depth and D) 8 m depth from 12:00 noon on 26th February to 2:00 pm on 28th February 2013. (See text for details). The start point for each plot is marked with a ⊗. ....38
- Figure 24.** Estimating the time lag for the mixing device current to be established after switch on. Date and time of turn of and establishment of the ADCP current 100 m from the mixing device are marked on both plots. ....39
- Figure 25.** Total nitrogen concentrations from the epilimnion (0.5 m) and hypolimnion (9 m) at Site 1 (mixing site) and Site 2 (control site) between 16 December 2011 and 13 June 2014. Open symbols indicate sampling periods when mixing devices were not operating. ....40

<b>Figure 26.</b> Total phosphorus concentrations from the epilimnion (0.5 m) and hypolimnion (9 m) at Site 1 (mixing site) and Site 2 (control site) between 16 December 2011 and 13 June 2014. Open symbols indicate sampling periods when mixing devices were not operating.....	41
<b>Figure 27.</b> Ammonium-nitrogen concentrations from the epilimnion (0.5 m) and hypolimnion (9 m) at Site 1 (mixing site) and Site 2 (control site) between 16 December 2011 and 13 June 2014. Schmidt stability is included for reference to potential lake stratification events. Open symbols indicate sampling periods when mixing devices were not operating.....	42
<b>Figure 28.</b> Nitrate-nitrogen concentrations from the epilimnion (0.5 m) and hypolimnion (9 m) at Site 1 (mixing site) and Site 2 (control site) between 16 December 2011 and 13 June 2014. Open symbols indicate sampling periods when mixing devices were not operating. ....	43
<b>Figure 29.</b> Dissolved reactive phosphorus concentrations from the epilimnion (0.5 m) and hypolimnion (9 m) at Site 1 (mixing site) and Site 2 between 16 December 2011 and 13 June 2014. Schmidt stability is included for reference to potential lake stratification events. Open symbols indicate sampling periods when mixing devices were not operating. Note: Dissolved reactive phosphorus concentration detection limit ( $0.004 \text{ mg L}^{-1}$ ). ....	44
<b>Figure 30.</b> Chlorophyll <i>a</i> monitoring data from BoPRC, 2009 to 2013. ....	45
<b>Figure 31.</b> Chlorophyll <i>a</i> at Site 1 (mixing site) and Site 2 (control site) in the epilimnion (0.5 m) and hypolimnion (9 m) between 16 December 2011 and 13 June 2014. Open symbols indicate sampling periods when mixing devices were not operating.....	46
<b>Figure 32.</b> Relative cell abundance of Site 1 (mixing site) phytoplankton taxonomic groups from the epilimnion (0.5 m) and hypolimnion (9 m) between 16 December 2011 and 13 June 2014. Dashed line indicates Schmidt stability calculated from CTD temperature data taken at time of sampling. Shaded sections indicate periods when mixing devices were in operation. Note that dinoflagellata, euglenophyta and chrysophyta have been omitted due to low abundance. ....	47
<b>Figure 33.</b> Relative cell abundance of Site 2(control site) phytoplankton taxonomic groups from the epilimnion (0.5 m) and hypolimnion (9 m) between 16 December 2011 and 13 June 2014. Dashed line indicates Schmidt stability calculated from CTD temperature data taken at time of sampling. Shaded sections indicate periods when mixing devices were in operation. Note that dinoflagellata, euglenophyta and chrysophyta have been omitted due to low abundance. ....	48
<b>Figure 34.</b> Total phytoplankton cell abundance in the epilimnion (0.5 m) and hypolimnion (9 m) of Site 1 (mixing site) and Site 2 between 16 December 2011 and 13 June 2014. Dashed line indicates Schmidt stability calculated from CTD temperature data taken at time of sampling. Shaded sections indicate periods when mixing devices were in operation. ....	49

<b>Figure 35.</b> Lake Rotoehu zooplankton group abundance for Site 1 (mixing site) epilimnion (0.5 m) and hypolimnion (9 m) between 16 December 2011 and 13 June 2014. Dash line indicates Schmidt stability calculated from CTD temperature data taken at time of sampling. Shaded sections indicate periods when mixing devices were in operation. ....	52
<b>Figure 36.</b> Lake Rotoehu zooplankton group abundance for Site 2 (control site) epilimnion (0.5 m) and hypolimnion (9 m) between 16 December 2011 and 13 June 2014. Dash line indicates Schmidt stability calculated from CTD temperature data taken at time of sampling. Shaded sections indicate periods when mixing devices were in operation. ....	53
<b>Figure 37.</b> Degree of similarity (Bray-Curtis) in plankton community composition between Site 1 (mixing site) and Site 2 (control site) for both the epilimnion (0.5 m) and hypolimnion (9 m) layers in Lake Rotoehu between 16 December 2011 and 13 June 2014. Shaded sections indicate periods when mixing devices were in operation. ....	55
<b>Figure 38.</b> Degree of similarity (Bray-Curtis) in plankton community composition between the epilimnion (0.5 m) and hypolimnion (9 m) layers of the Site 1 (mixing site) and Site 2 (control site) locations in Lake Rotoehu between 16 December 2011 and 13 June 2014. Shaded sections indicate periods when mixing devices were in operation. ....	56

## List of tables

<b>Table 1.</b> Operational log of Lake Rotoehu mixing devices. ....	21
<b>Table 2.</b> Analysis of Lake Rotoehu phytoplankton taxonomic group abundance. Data were allocated to periods when either the mixing devices were operating (ON) or shut down (OFF); Student's t-tests were then conducted between the mixing site (Site 1) and control site (Site 2) and between two depths, the epilimnion (0.5 m) and the hypolimnion (9 m). Means that are significantly different are presented in bold. ....	50
<b>Table 3.</b> Analysis of Lake Rotoehu zooplankton taxonomic group abundance. Data were allocated to periods when either the mixing devices were operating (ON) or shut down (OFF); Student's t-tests were then conducted between the mixing site (Site 1) and control site (Site 2) and between two depths, the epilimnion (0.5 m) and the hypolimnion (9 m). Means that are significantly different are presented in bold. ....	54

## Introduction

### Threats to lake systems

Lake ecosystems provide valuable services, including water regulation, nutrient cycling, supply of food resources, and cultural and conservation values (Wetzel 2001). Healthy lake systems often provide important economic and cultural contributions through increased property values, income from recreation and tourism, and maintenance of intrinsic and aesthetic values. Changes in human land use in lake catchments can accelerate the process of eutrophication, thus reducing the ability of ecosystems to provide these services (Wilcock et al. 2006).

Aquatic ecosystem health can be threatened by increases in external nutrient loads associated with catchment land uses including agriculture and urban development. Losses of nitrogen and phosphorus from land over and above natural (non-anthropogenic) levels can increase primary production and trophic state (i.e., induce eutrophication). Eutrophic systems are typified by poor water quality and blooms of cyanobacteria that reduce ecosystem services and can be a threat to human and animal health (Wetzel 2001; Abel et al. 2010). Many eutrophic systems also receive 'internal loading' of nutrients from bottom sediments, through wind-driven resuspension of sediment in shallow areas and/or release (desorption) due to hypoxic conditions near the sediment-water interface, generally in deeper waters (Jeppesen et al. 2005; Søndergaard et al. 2010).

Thermal stratification occurs when surface waters (the epilimnion) are warmed by the sun, forming a stable layer above colder, denser water near the lake bottom (hypolimnion). This density gradient prevents mixing of surface and bottom waters (Drake & Harleman 1969). Respiration of organisms during decomposition of organic matter in the isolated hypolimnion consumes dissolved oxygen. In eutrophic systems, bottom waters may become hypoxic or anoxic, resulting in phosphate bound to the sediment being released into the water column (Wetzel 2001). Ammonium may also build up with hindrance of nitrification (Ashley 1983a). These nutrients can support additional growth of phytoplankton, particularly as nutrients are redistributed through the euphotic zone. Furthermore, isolation of surface waters can provide a competitive advantage to cyanobacteria, due to their buoyancy, aiding growth rates at elevated temperatures, and the capacity of some species to utilise atmospheric nitrogen for growth (Oliver et al. 2012).

### Lake Rotoehu

Rotoehu is a shallow (mean depth 8.2 m), moderately sized (c. 795 ha), polymictic lake (i.e. multiple incidences of water column mixing within a year) in the northeast of the

Rotorua/Te Arawa lakes district (Scholes & Bloxham 2008). The catchment land use is relatively evenly distributed between exotic forestry, native vegetation and pasture (Scholes 2009), and there are small human settlements at Ngamimiro Bay and Otautu Bay on the eastern side of the lake. Inflow to the lake is from small surface streams, groundwater and geothermal springs (Donovan, 2003). Geothermal waters contribute concentrated inputs of dissolved nitrogen and phosphorus to the lake (Scholes 2009). The trophic state of the lake has historically been classified as mesotrophic to eutrophic (Jolly & Chapman 1977; Scholes 2009). The Trophic Lake Index (TLI) of the lake increased dramatically in the early 1990s, and was high but stable (c. 4.5) between 1994 and 2009 (Scholes 2009). Associated with elevated TLI, cyanobacteria blooms have occurred regularly since 1993. The Lake Rotoehu Action Plan was therefore formulated to help achieve a three-year average TLI target of 3.9 (BoPRC, 2007).

Bay of Plenty Regional Council (BoPRC) has undertaken several initiatives to improve the water quality of Lake Rotoehu. These include the improvement of land management practices to reduce nutrient losses from pasture, installation of an alum treatment facility at the Waitangi Soda Spring inflow to the lake, construction of a floating wetland and regular harvesting of submerged vegetation from the lake. These combined initiatives coincide with improvements in water quality from 2007 to present, with the target three-year TLI nearly achieved in 2013 (Figure 1) (Scholes 2009).

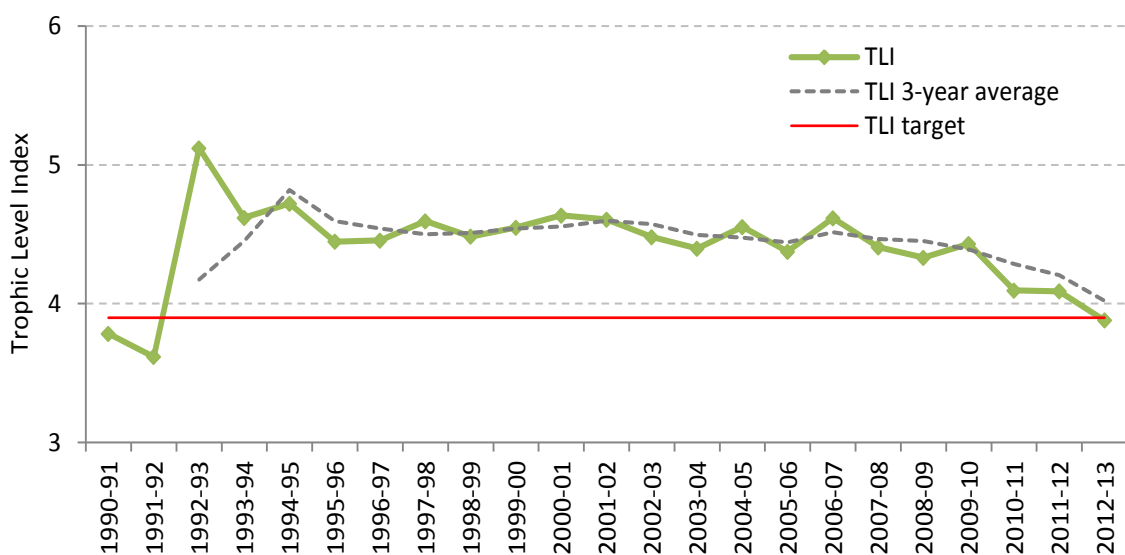


**Figure 1.** Historical Trophic Level Index (TLI) of Lake Rotoehu from 1991 to 2013 (BoPRC).

### Artificial destratification

Despite recent water quality improvements in Lake Rotoehu, the proliferation of buoyant cyanobacteria remains of concern. To that end, BoPRC commissioned the

design and installation of two mixing devices (Del Monte Ltd, Tauranga) for Lake Rotoehu. The devices were designed to increase natural mixing between surface and bottom waters in order to reduce or prevent stratification and limit occurrences of bottom-water hypoxia. Mixing of surface and bottom water also has an added benefit of disrupting accumulations of buoyant cyanobacteria, further mitigating harmful blooms (Heo & Kim 2004).

Installation of two mixing devices in the lake was completed in November 2012. Each device was supplied with compressed air from a shore-based station on the southern edge of the lake. Compressed air was released through a diffuser into three columns (2.2 m in diameter) with a 5.0 m vertical section, entraining water from the hypolimnion as the bubbles rose to the surface. The top of each column had a 90° bend to direct the upwelling water horizontally into the epilimnion. Each device was theoretically capable of moving 15,000 m<sup>3</sup> h<sup>-1</sup> of water. Following the first season of operation (summer 2013) the devices were modified to reduce blockages caused by lake weeds and improve performance. Although no direct quantification of device performance was conducted during the second season of operation (summer 2014), visual assessments of the devices supported improved performance following the modifications.

Several studies have evaluated the efficacy and impacts of artificial lake destratification using mathematical modelling and biological surveys (Miles & West, 2011; Toffolon & Serafini, 2013), but few have investigated the effect of artificial mixing on lakes as large as Rotoehu. Artificial mixing has been reported as having both phytoplankton species-dependent positive and negative effects. For example, the filamentous diatom *Melosira italica* usually disappears during summer stratification of Blelham Tarn, England, due to high sedimentation losses to the hypolimnion (Lund 1971). Lund (1971) documented the presence of this species during the summer of 1967, however, when the lake was mixed artificially in the late summer of 1967, the population of *M. italica* increased and persisted into the following year rather than declining in the late summer. In another case, cyanobacteria populations were shown to be inhibited and replaced by diatoms using artificial mixing in Lake Dalbang (South Korea) (Heo & Kim 2004). Zooplankton populations appear to be less influenced by artificial mixing, with changes in population structure more closely associated with changes in food availability (Lackey 1973; McClintock & Wilhm 1977; Ashley 1983b).

The University of Waikato (UoW) was contracted to monitor phytoplankton and zooplankton communities concurrently with artificial mixing in Lake Rotoehu. A variety of methods was used to evaluate the effects of the artificial mixing devices, including measurements of physical and chemical variables. A dye tracer study was undertaken by the National Institute of Water and Atmospheric Research Ltd (NIWA) to trace the movement of the water plume arising from one of the mixing devices.

This report presents the biological, physical and chemical monitoring results in Lake Rotoehu from December 2011 to June 2014, along with recommendations for further data collection and monitoring. Results from the study may help to inform revisions of restoration initiatives at the lake, and aid the design of similar artificial mixing and nutrient management programs in other lakes.

## Methods

### Site description

Measurement sites were selected to represent some of the spatial variability around Lake Rotoehu, both in close proximity to, and at distance from the two mixing devices. Figure 2 shows the locations of the water sampling sites and Bio-Fish transect path. Mixing devices were installed centrally in the lake. The water column profiling monitoring buoy was installed approximately 100 m from the southern mixing device. The mixing site (Site 1) was located approximate 30 m from the southern mixing device while the control site (Site 2) was selected to be as far from the mixing devices but still in the same depth of water (9-10 m, depending on lake water level).

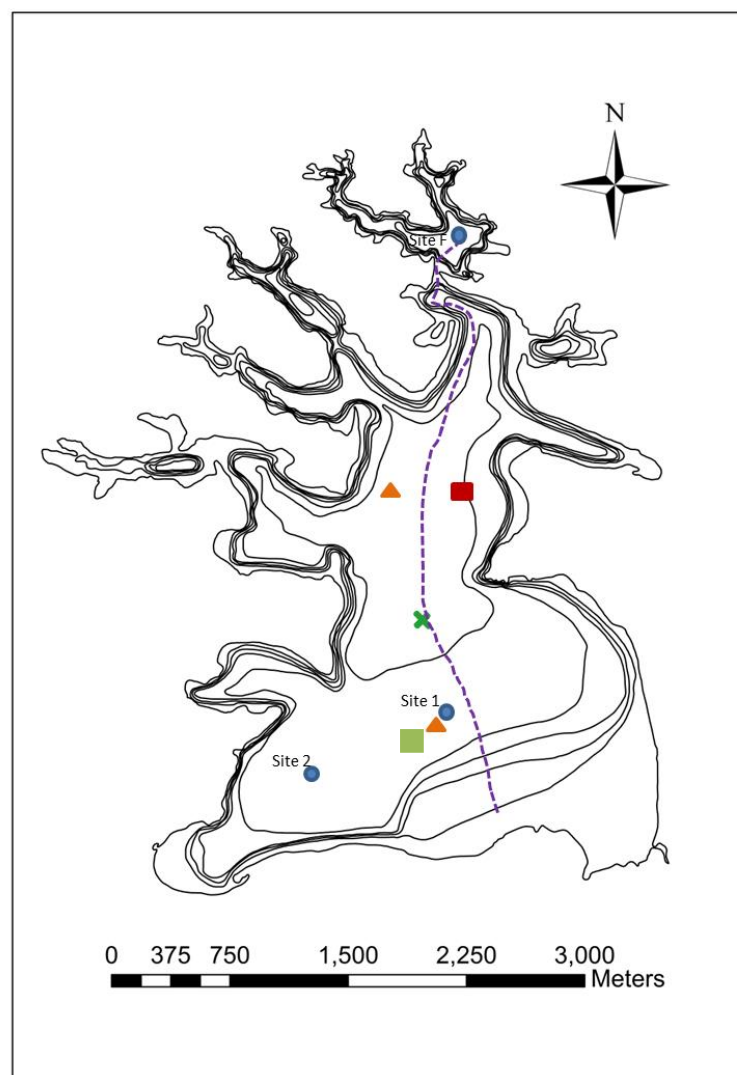


**Figure 2.** Map of Lake Rotoehu showing sampling locations. Destratification devices are represented by orange triangles. Blue circles represent sampling locations. The profiler buoy is also located at sampling Site 1. The green cross marks the location of the primary (central lake) BoPRC monitoring site. The fixed sensor monitoring buoy location is represented by the red square and profiling buoy location with a green square. The purple dashed line indicates the route taken (south to north) during Bio-Fish surveys which ended at Site F.



## Meteorology

Meteorological data were obtained from the Rotorua Airport climate station administered by the New Zealand Meteorological Service and obtained via the National Institute of Water and Atmospheric Research's (NIWA) 'cliflo' database (<http://cliflo.niwa.co.nz>). Daily mean values were calculated from hourly measurements of short wave radiation, air temperature, vapour pressure, wind speed, and daily total rainfall was calculated for rainfall, for the period January 2009 to December 2013.

## Monitoring buoy – fixed sensors

The University of Waikato and BoPRC installed a water quality monitoring buoy in central Lake Rotoehu in April 2011. The buoy collects quarter-hourly data for meteorological (air temperature, wind speed and direction, humidity, barometric pressure, and rainfall) and water quality (chlorophyll fluorescence, dissolved oxygen, and water temperature) variables. Data are sent via cellular telemetry and posted in near real-time to the Bay of Plenty Regional Council website. The buoy measures water temperature at seven depths, and dissolved oxygen at the surface and bottom of the water column. It thus provides a comprehensive, high-frequency record of thermal and dissolved oxygen dynamics in the lake. The monitoring buoy is located between the two mixing device locations and thus its measurements are not influenced by the mixing effects visible in the immediate vicinity of either machine.

Water column temperature measurements from the buoy were used to calculate a daily average 'Schmidt Stability Index' using the software 'Lake Analyzer' (Read et al. 2011). This index describes the energy potentially required to mix surface and bottom waters to achieve homogeneous density (i.e. no vertical thermal gradient) and is a measure of the strength of thermal stratification.

## Monitoring buoy – Water column profiling sensors

In order to provide further insight into Lake Rotoehu dynamics, and specifically the effects of the mixing devices on the water column, a second monitoring buoy was installed in June 2013 c. 100 m from mixing site (Site 1) (Figure 2). The buoy used an automated winch to raise and lower a water quality sensor package in order to measure water temperature, dissolved oxygen, and chlorophyll fluorescence at a two-hour interval and at c. 0.5 m increments through the water column.

## CTD Profiles

Water column profiles were taken monthly at sites A and B between December 2011 and June 2014, using a conductivity-temperature-depth (CTD) profiler (SBE 19 plus SEACAT Profiler, Seabird Electronics Inc.), with additional mounted sensors for dissolved oxygen (DO) concentration (Seabird Electronics), chlorophyll fluorescence (Chelsea MiniTracka II) and beam transmittance (WetLabs C-star).

### Bio-Fish

The Bio-Fish is a towed probe that measures water temperature, conductivity, dissolved oxygen, chlorophyll fluorescence, and photosynthetically active radiation. The instrument records these values, along with a corresponding depth reading and GPS location at a frequency of 4 Hz as it is towed through the water from a boat (Figure 3). As the Bio-Fish moves through the water, it is guided manually along an undulating path, sampling all depths through the water column. The horizontal aspect of the Bio-Fish transect undertaken in Lake Rotoehu is presented in Figure 2.

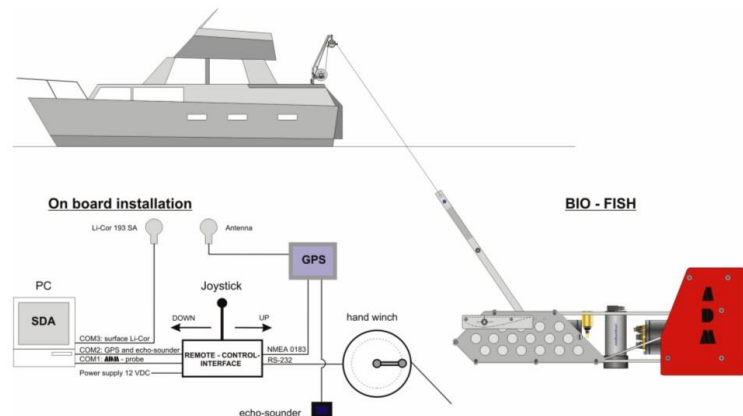


**Figure 3.** Illustration of Bio-Fish set-up. The size of the boat has been scaled down approximately 10-fold compared with the Bio-Fish device and on-board installation.

### Chlorophyll, nutrients and Secchi disk depth

Water samples were collected for analysis of chlorophyll *a*, total nutrients (nitrogen and phosphorus), dissolved nutrients (dissolved reactive phosphorus, ammonium, nitrate and nitrite) from the epilimnion (0.5 m) and hypolimnion (9 m) at Site 1 (mixing site) and Site 2 (control site) (see Figure. 2) in Lake Rotoehu from December 2011 to June 2014 (see Appendix 1.5 for sampling dates). Water column profiles of dissolved oxygen, temperature and conductivity were also collected using a Sea-Bird CTD instrument at Site 1 and Site 2 from December 2011 to June 2014. Water clarity was measured using a Secchi disk comprising a 20-cm diameter disk with black and white markings which is lowered into the water until no longer visible. Secchi disk measurements were combined with the historical record from BoPRC.

### Dye tracer study

On 27 February 2013, NIWA and BoPRC initiated a dye tracer study using Rhodamine WT to colour the water. The dye was injected inside the northern arm of the southern mixing device assembly at the bottom of the diffuser to allow the dye to mix within the riser before emerging in the lake. A total of about 8 L of 20% Rhodamine WT dye, diluted to 5% (50 g L<sup>-1</sup>) for handling, was dispensed from a metering pump at a delivery rate of

120 mL min<sup>-1</sup> over a period of 1 hour. The pump and dye were deployed from a small aluminium dinghy tethered to the mixing device surface buoys.

Measurement of the dye was achieved using a hand operated Seapoint Rhodamine fluorescence probe, which was vertically profiled at GPS-referenced points along the flow path of the visible plume and beyond, to a distance of 100 m from the mixing device.

### **Current measurements**

As part of the dye tracer study in February 2013, NIWA deployed a bottom-mounted Acoustic Doppler Current Profiler (ADCP, Seapoint) in line with the observed dye plume at 100 m from the mixing device. A second ADCP was used from a boat, in bottom-tracking mode, as a mobile current profiler circling the mixing device assembly, to assess current plumes from all three outlets from the mixing device. The bottom-mounted ADCP was set to measure current speed and direction as the mean of 500 pings and the bottom tracking ADCP measured a current speed and direction profile (ensemble) programmed to link with the GPS location of the boat and corrected for the movement of the boat relative to the lake bed. Both ADCPs measured in 1-m bins although currents could not be measured closer than 1.3 m from the lake bed or 1 m from the lake surface.

The bottom-tracking ADCP was moved around the mixing device in several circuits of increasing diameter to map the extent of the current plumes from each of the three outflows from the mixing device. The bottom-mounted ADCP was left in position for two weeks after the mixing device was turned off, to assess the decay rate of any currents produced by the mixing device, to define natural background lake currents and to determine how rapidly any currents were established when the mixing device was turned on again.

### **Plankton community sampling**

Phytoplankton and zooplankton samples were collected at depths of 0.5 m and 9.0 m at Sites 1 and 2 from December 2011 to June 2014 (see Appendix 1.5 for sampling dates) using a 10 L Schindler-Patalas trap. Unfiltered phytoplankton samples (400 mL) were preserved with Lugol's iodine, while zooplankton were collected by filtering 10 L of lake water through a 40 µm net with the trapped sample preserved with 70% ethanol.

Phytoplankton analyses were carried out using Utermöhl settling chambers (Utermöhl, 1958) and an inverted microscope (Olympus, Ix71, Japan). Phytoplankton were identified to genus level, and relative abundance was determined for each phylum. Enumeration of phytoplankton (cells mL<sup>-1</sup>) used methods adapted from Hötzel & Croome (1999) and US Environmental Protection Agency (2007). A 10 mL subsample was settled in an Utermöhl chamber. Phytoplankton were counted at 4000 or 2000

times magnification in a single transect, including at least 100 planktonic units (cells, colonies and filaments) of the dominant species.

Zooplankton were identified and enumerated by passing samples through a 40- $\mu$ m mesh to remove ethanol solution and to attain a final known volume, dependant on abundance. Samples were enumerated in 5 mL aliquots in a gridded Perspex tray until at least 300 individual counts were obtained or the entire sample was enumerated. Species were identified using standard guides (e.g., Chapman & Lewis, 1976; Shiel 1995).

Plankton community composition was quantified using the Bray-Curtis similarity metric using PRIMER v.6. Similarity is given along the range from 0 (completely dissimilar) to 100 (exact similarity). Data were grouped by sampling site and depth and matched by sampling date. Further analysis was performed on  $\log(x+1)$ -transformed abundance counts.

### **Mixing device operation**

The two mixing devices were installed in July 2012 (Figure 4), and turned off during from June to November 2013. Following repairs and modifications they were operated continuously from December 2013 to the end of May 2014. During the first summer of operation the devices were turned off for two periods of maintenance and for two weeks in early March as part of the study involving current measurements. Timing of device operation is given in Table 1. Measurements of flow rates and observations by divers during the first summer (2012–13) indicated that flow rates were often sub-optimal due to interference by weed rafts and/or machine imbalances. During the second summer (2013–14) operational efficiency and flow rates were improved by the removal of the intake grates originally intended to prevent weed from being drawn into the device.



**Figure 4.** Installation of the mixing devices in Lake Rotoehu. Images by A. Bruere.

**Table 1.** Operational log of Lake Rotoehu mixing devices.

Event	Start	End	Action
Commissioning	Jul 2012		Machines deployed and turned on
Mooring maintenance	mid-Oct 2012	24 Nov 2012	Machines turned off to adjust screw anchors
Machine failure	11 Dec 2012	13 Dec 2012	Machines off due to equipment failure
Survey	28 Feb 2012	16 Mar 2013	Both machines turned off for ADCP currents study
Winter/machine modifications	09 Jun 2013		Machines decommissioned for winter and upgrades
Summer 2013-2014	mid-Nov 2013		Machines turned on and run continuously
Winter/machine modifications	end May 2014		Machines decommissioned for winter and upgrades

## Results

### Monitoring buoy – fixed sensors

Monitoring buoy data show fluctuations in water temperature, with strong stratification events during the 2011-2012, and 2012-2013 summers, but also weaker stratification events occurring as early as August in 2012. In December 2012 and January 2013 temperatures were warmer than the previous summer, and there were several periods of sustained strong stratification (Figure 5). During these events, dissolved oxygen levels in the hypolimnion reached minima of close to 10% saturation (Figure 6). The Schmidt stability index, calculated in part from the temperature profiles, confirmed that stratification was generally stronger (i.e., higher values of the index) and more sustained in 2012/13 than in 2011/12 summer period (Figure 7).

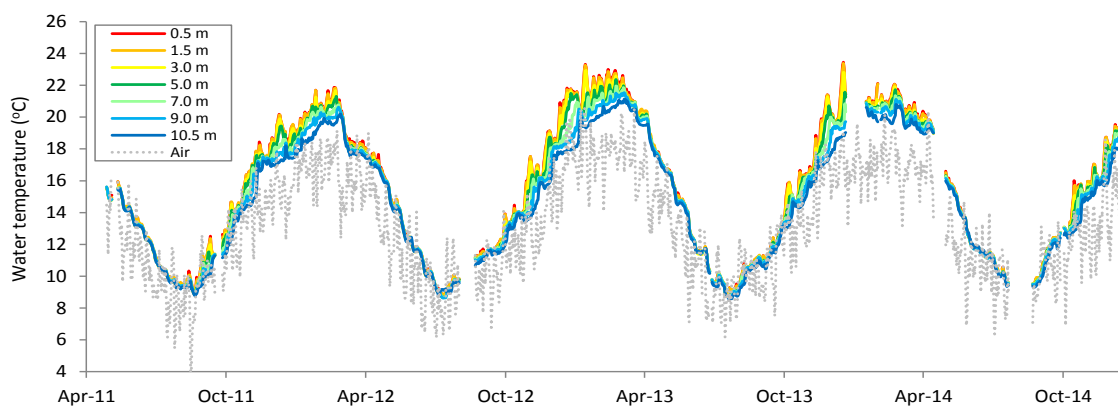


**Figure 5.** Temperature of air and water at different depths based on records from the Lake Rotoehu monitoring buoy for the period April 2011 to December 2014.

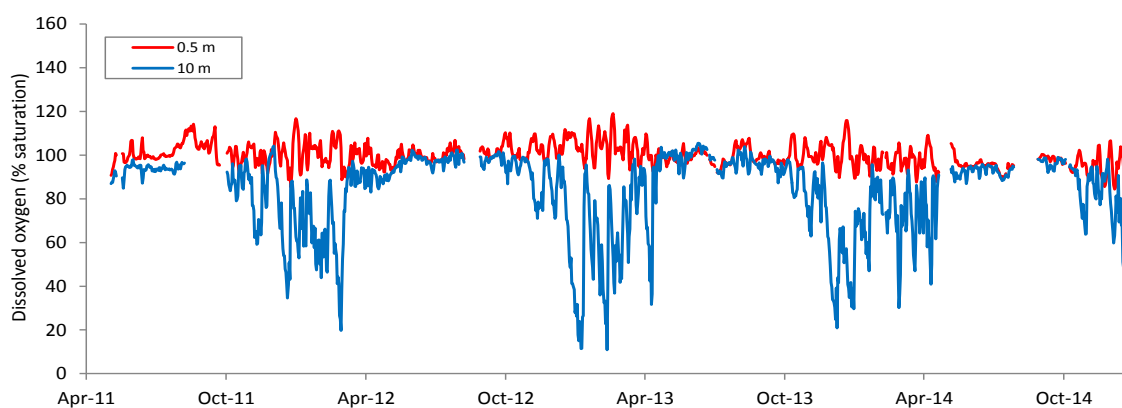


**Figure 6.** Percent saturation of dissolved oxygen at two depths, based on records from the Lake Rotoehu monitoring buoy for the period April 2011 to December 2014. Sections of data have been corrected for electronic sensor drift.



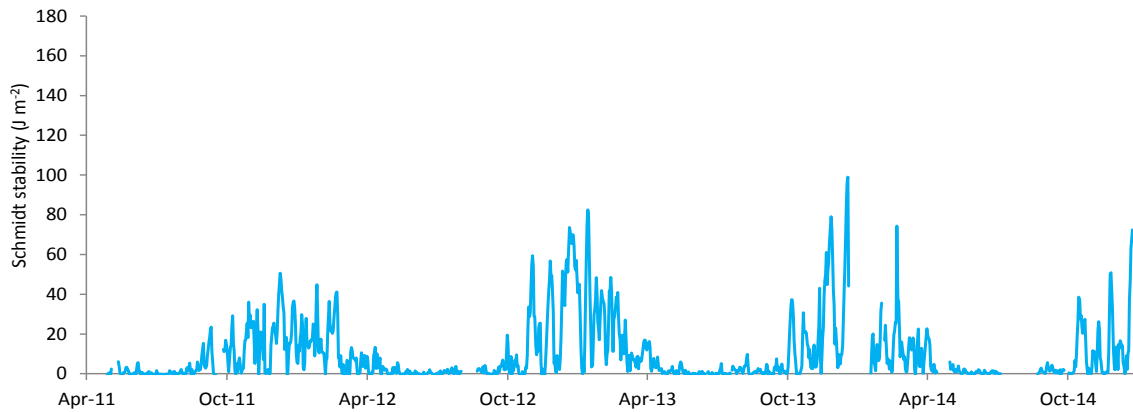


**Figure 7.** Schmidt stability index of Lake Rotoehu, based on records from the Lake Rotoehu monitoring buoy for the period April 2011 to December 2014. A higher Schmidt stability value indicates stronger stratification of the water column.

### Profiler Buoy

The UoW prototype profiler buoy was installed and fully operational c. 100 m from the southern mixing device from September 2013 (Figure 2). Periods of stratification lasting several days were observed from January to March 2014 (Figure 8) and this was associated with slight oxygen depletion in the bottom waters (Figure 9). A minimum safety margin of between 1 and 1.5 m from the bottom (as detected by the depth sounder) for the profiler meant oxygen depletion near the sediment water interface may have been more severe than observed by the profiler. Future operation of the profiler will reduce this safety margin in order to collect profiles closer to the bottom sediments. No oxygen depletion was observed during periods of winter mixing.

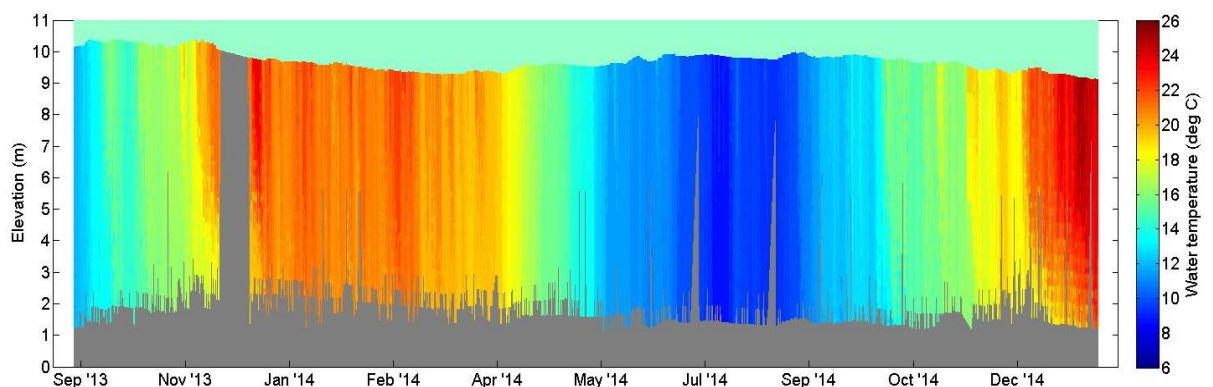


**Figure 8.** Water temperature at different depths in Lake Rotoehu as measured by the profiler buoy between September 2013 and December 2014. Areas of grey represent insufficient resolution to allow interpolation of temperature.

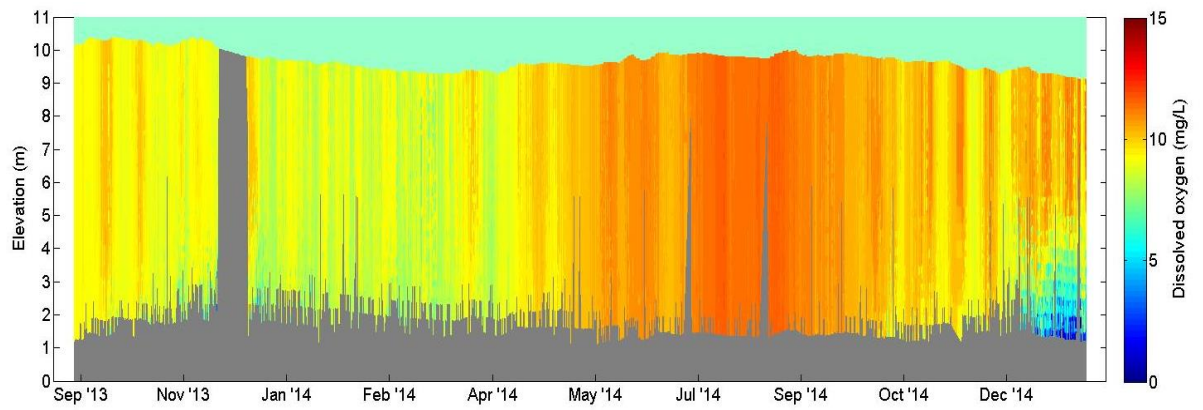


**Figure 9.** Dissolved oxygen concentration at different depths in Lake Rotoehu as measured by the profiler buoy between September 2013 and December 2014. Areas of grey represent insufficient resolution to allow interpolation of dissolved oxygen.



### Meteorological data

Weather is the main driver of lake stratification, and can be a confounding variable in a multi-year study where it is desired to isolate other anthropogenic drivers. Notably, 2011-2012 was an unusually cold and wet year while 2012-2013 and 2013-2014 were hot and dry (Figure 10).

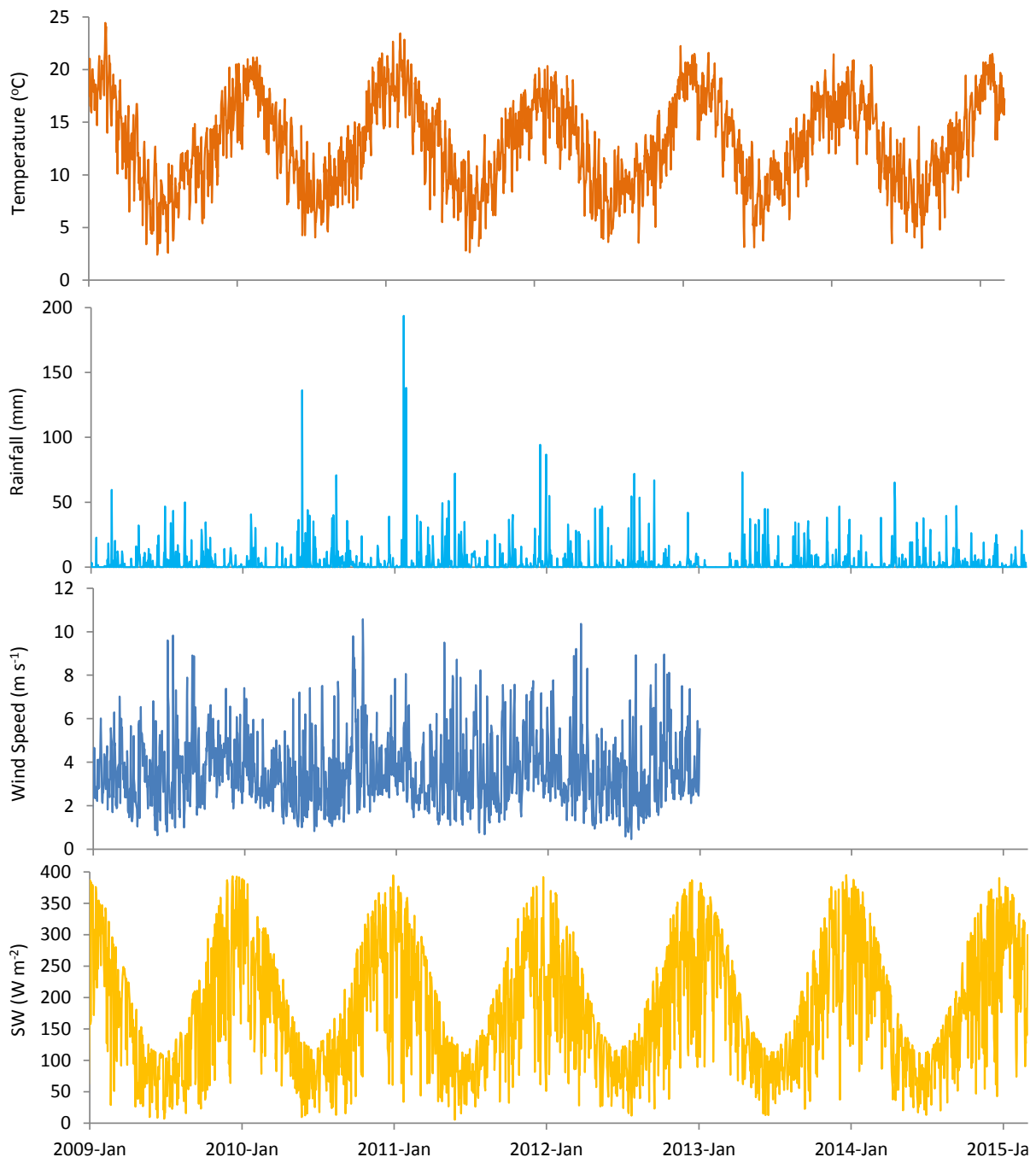


**Figure 10.** Meteorological data from January 2009 to January 2015, including short wave radiation (SW), air temperature, vapour pressure, wind speed, atmospheric pressure and rainfall. Data were obtained from the Rotorua Airport climate station via the cliflo database ([cliflo.niwa.co.nz](http://cliflo.niwa.co.nz), station number 1770) with daily means calculated from hourly measurements.

### CTD and Bio-fish profiles

Water column CTD (conductivity-temperature-depth) profiles were taken at two sites in Lake Rotoehu on 32 occasions between December 2011 and June 2014. Site 1 (mixing site) was located adjacent to the southern mixing device whereas Site 2 (control site) was located c. 400 m away (Figure 2).

Prior to the installation of the mixing devices, water temperature profiles at the two sites were very similar on all sampling occasions, with the possible exception of 21 August 2012, when a weak thermocline at site B was not observed at site A (Figure 12). On many occasions following commissioning of the mixing devices, the water column was well mixed throughout the lake, precluding detection of effects by the mixing device. However, on several occasions when there was some stratification, the water column near the mixing device was more deeply mixed than that at site B, specifically 29 Nov 2012, 17 Jan 2013, 22 February 2013 and 18 December 2013 (Figures 11–14). These observations suggest that the mixing devices were capable of influencing the strength of stratification in the immediate area of the device, although the effects were reduced rapidly with distance from it.

A Bio-Fish transect (Figure 2) was undertaken on 20 occasions between 18 November 2011 and 21 March 2013 (Figures 15–18). A large amount of data was generated from these transects and only selected examples are presented here. These observations show that the vertical temperature structure obtained from CTD casts are representative of almost the entire lake. During most of the year, the majority of the lake is well mixed in the vertical with high oxygen concentration to the bottom of the biofish track. Only the northern basin, which is separated from the rest of the lake by a shallow and narrow connection, shows more persistent stratification and low oxygen concentration in the hypolimnion (Figure 15, Figure 18). The summer surveys showed that the stratification and bottom-water hypoxia seen in the CTD profiles generally extend over the entire lake (Figure 16, Figure 17), but they also demonstrate important features in horizontal variability through the lake, such as the tilted thermocline on 22 February 2013 (Figure 17). The transects highlight the importance of quantifying horizontal variability in water column structure in order to distinguish effects of destratification devices from natural phenomena such as seiches and internal waves. Also notable is the frequent disconnect between the very small northern basin and the main lake. The northern basin was frequently more stratified, had higher water clarity, and may have been more strongly influenced by inputs from groundwater sources.

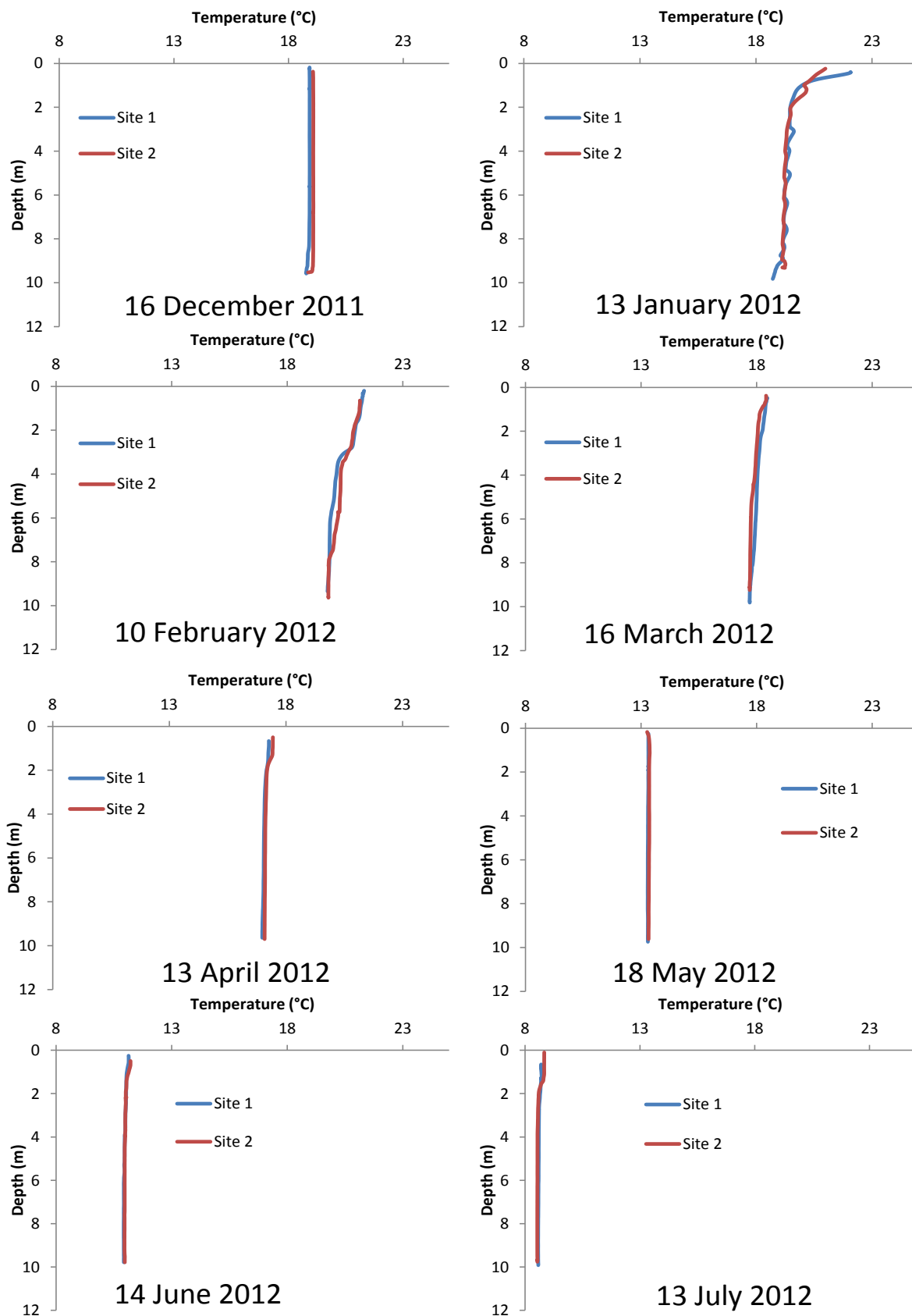


**Figure 11.** Comparison of CTD casts taken at Site 1 (mixing site) and Site 2 (control site) (c. 400 m from mixing device). Casts presented are prior to installation of the mixing devices.

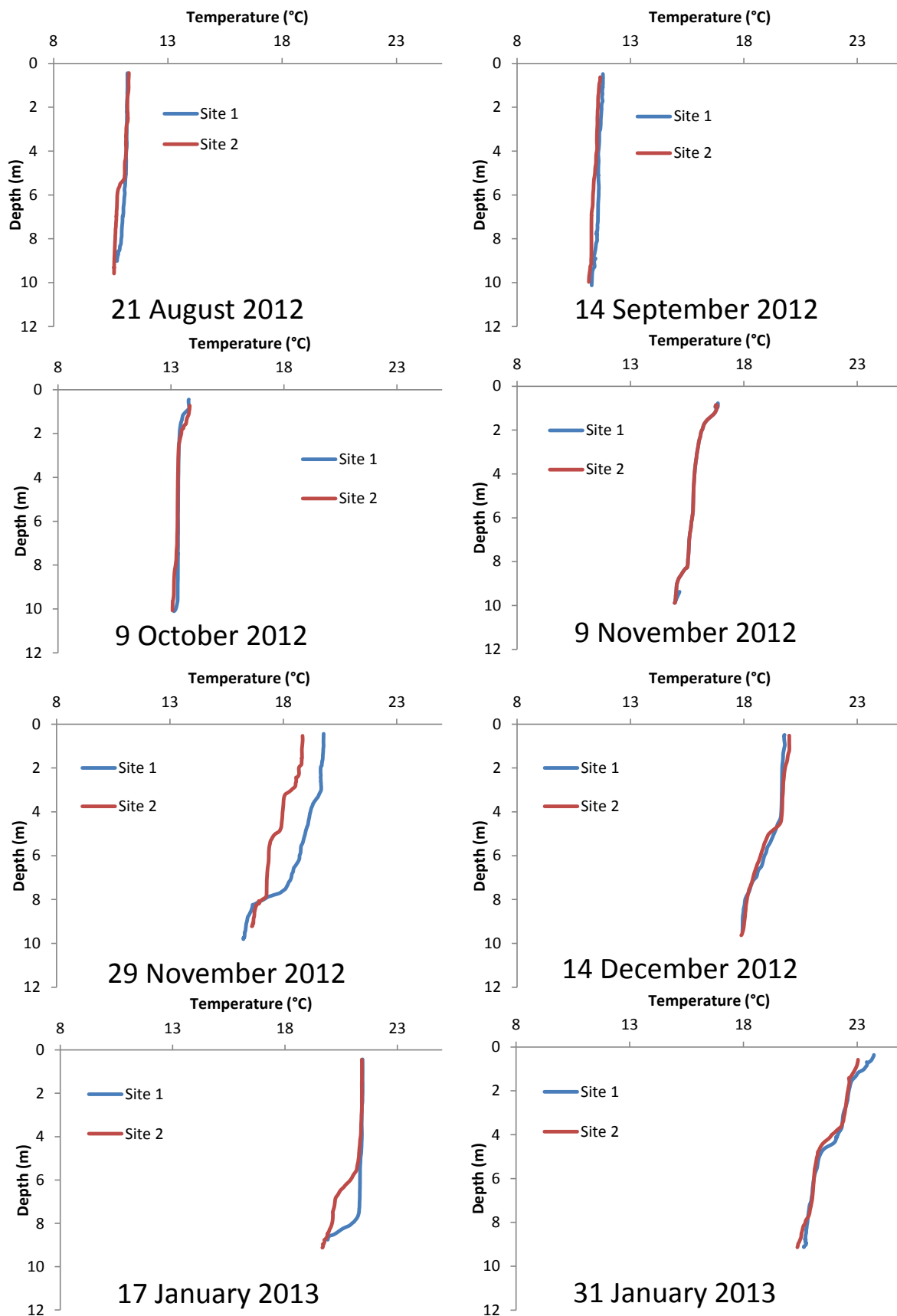


**Figure 12.** Comparison of CTD casts taken at Site 1 (mixing site) and Site 2 (control site)(c. 400 m from mixing devices). The mixing devices were active from mid-November 2012.

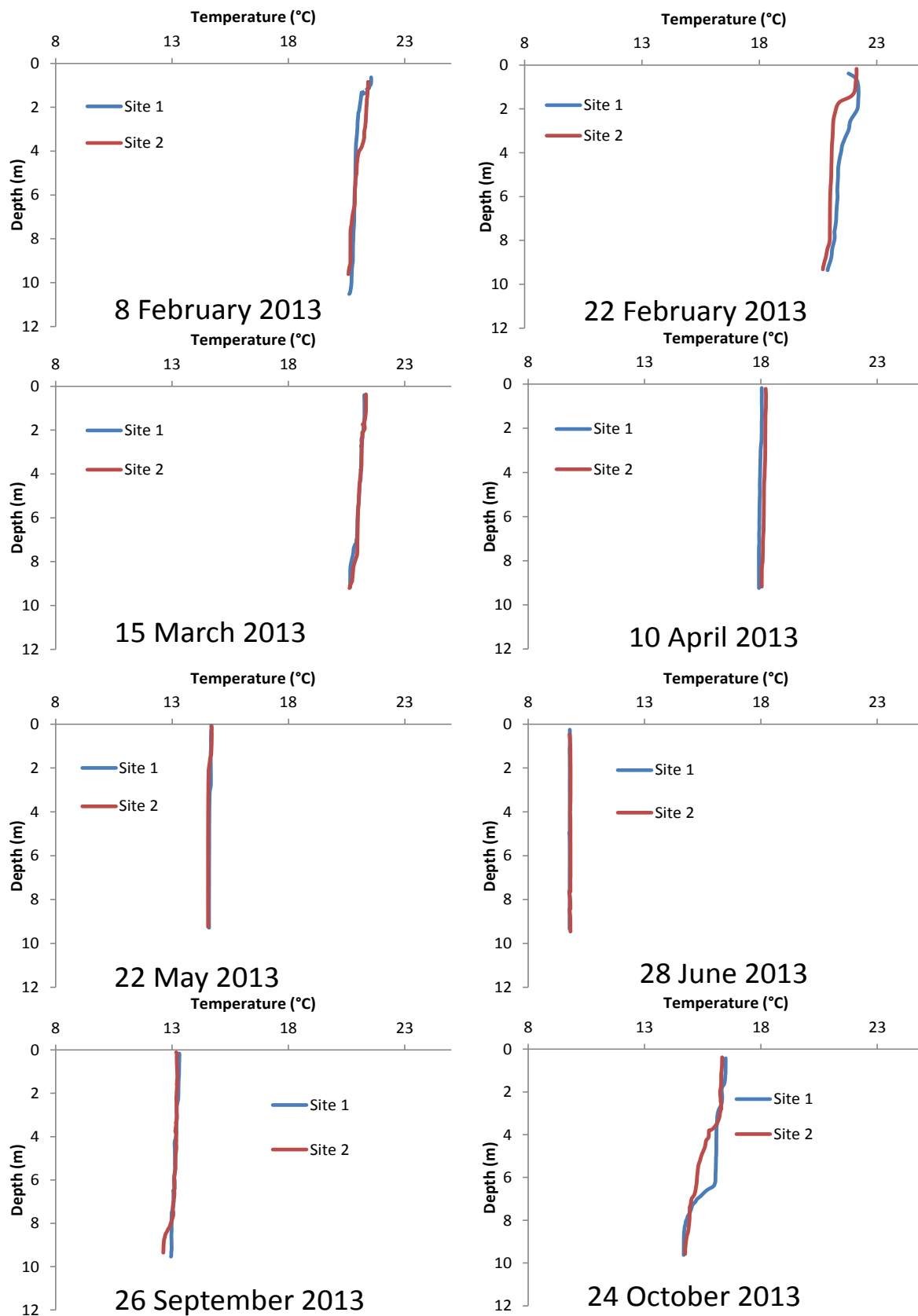


**Figure 13.** Comparison of CTD casts taken at Site 1 (mixing site) and Site 2 (control site) (c. 400 m from mixing devices). The mixing devices were not in operation on 15 March, 28 June, 26 September and 24 October 2013.

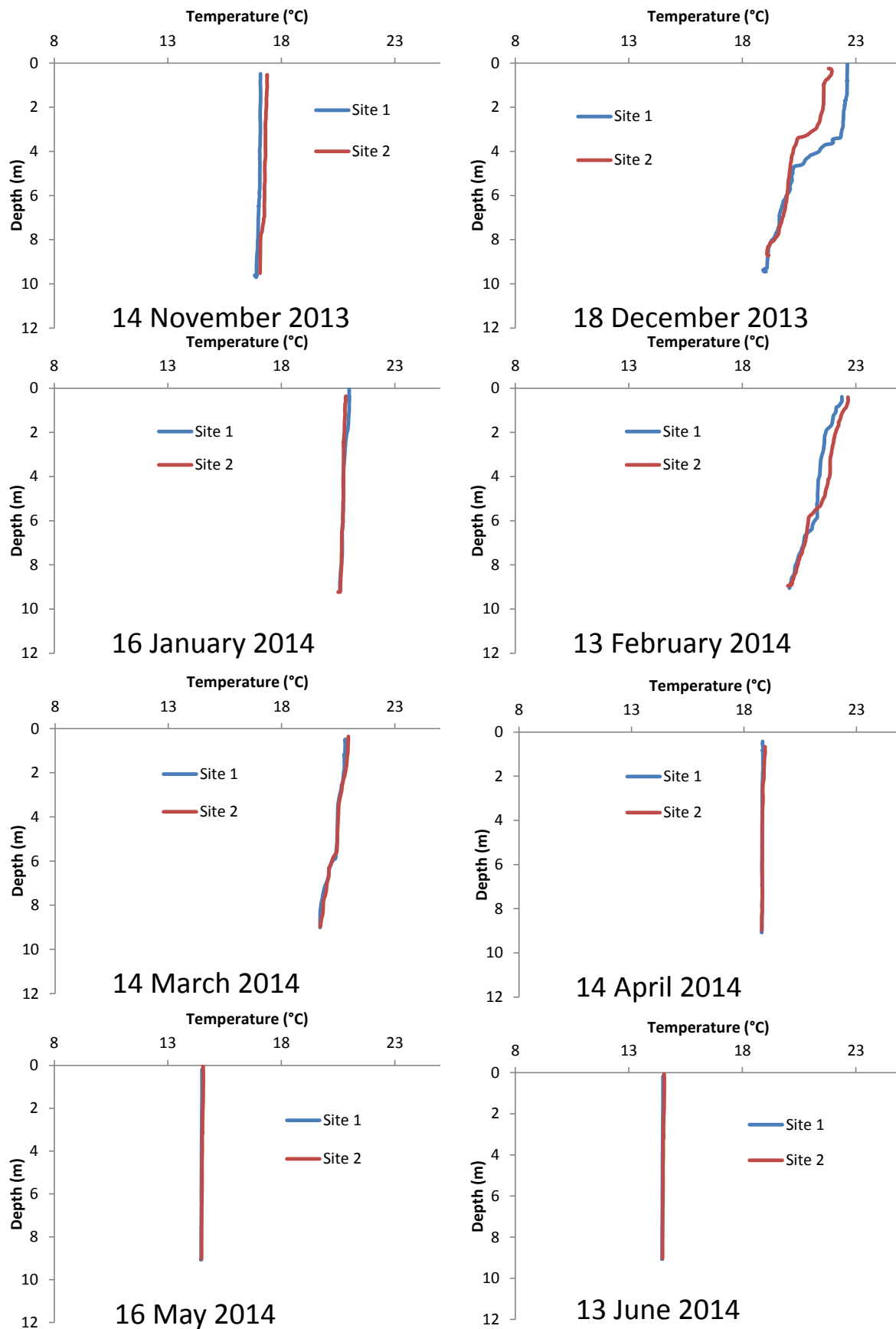


**Figure 14.** Comparison of CTD casts taken at Site 1 (mixing site) and Site 2 (control site) (c. 400 m from mixing device). Mixing devices were in operation from 14 November 2013 to 13 June 2014.

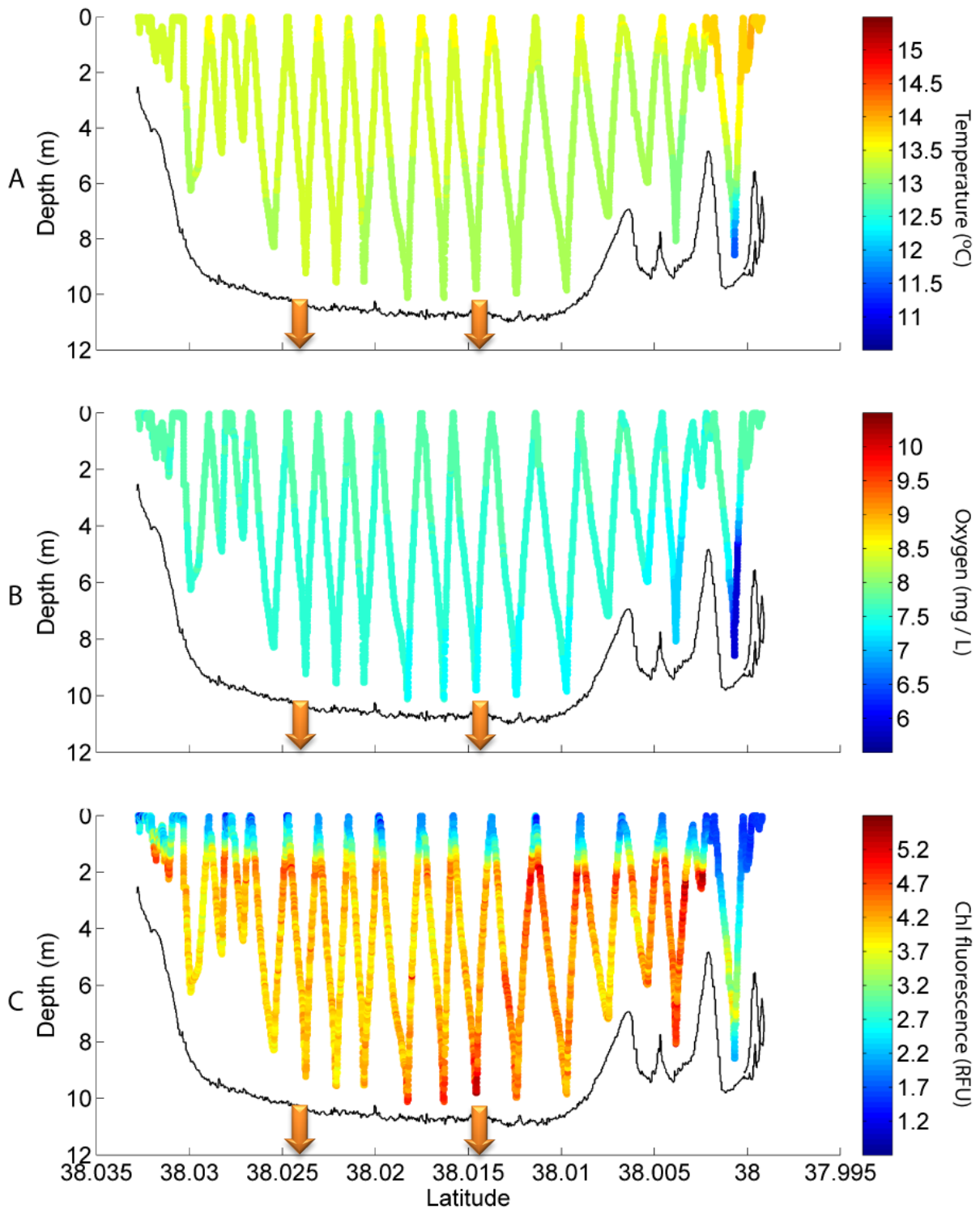


**Figure 15.** Cross-section of Lake Rotoehu showing the undulating path of the Bio-Fish device from south (left) to north (right) through the water on 9 October 2012 for A) water temperature, B) dissolved oxygen concentration, and C) chlorophyll fluorescence. Fluorescence data are reduced near the water surface, likely indicating non-photochemical quenching (bright-light inhibition of phytoplankton fluorescence response). Orange arrows denote the location of the mixing devices. The Bio-Fish passed within 100 m of the southern machine, and approximately 350 m from the northern machine (see Figure 2).

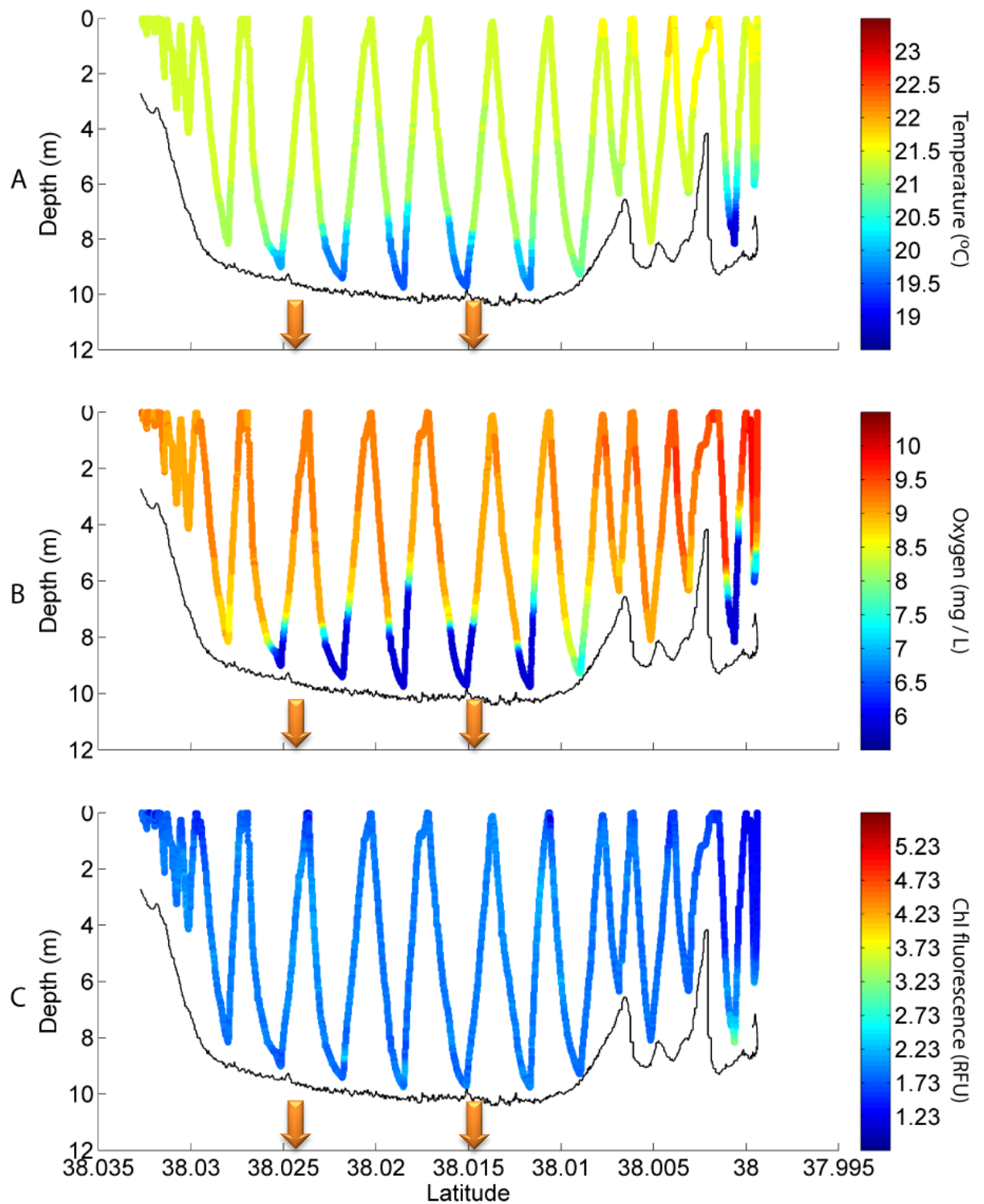


**Figure 16.** Cross-section of Lake Rotoehu showing the undulating path of the Bio-Fish device from south (left) to north (right) through the water on 17 January 2013 for A) water temperature, B) dissolved oxygen concentration, and C) chlorophyll fluorescence. Orange arrows denote the location of the mixing devices. The Bio-Fish passed within 100 m of the southern machine, and approximately 350 m from the northern machine (see Figure 2).



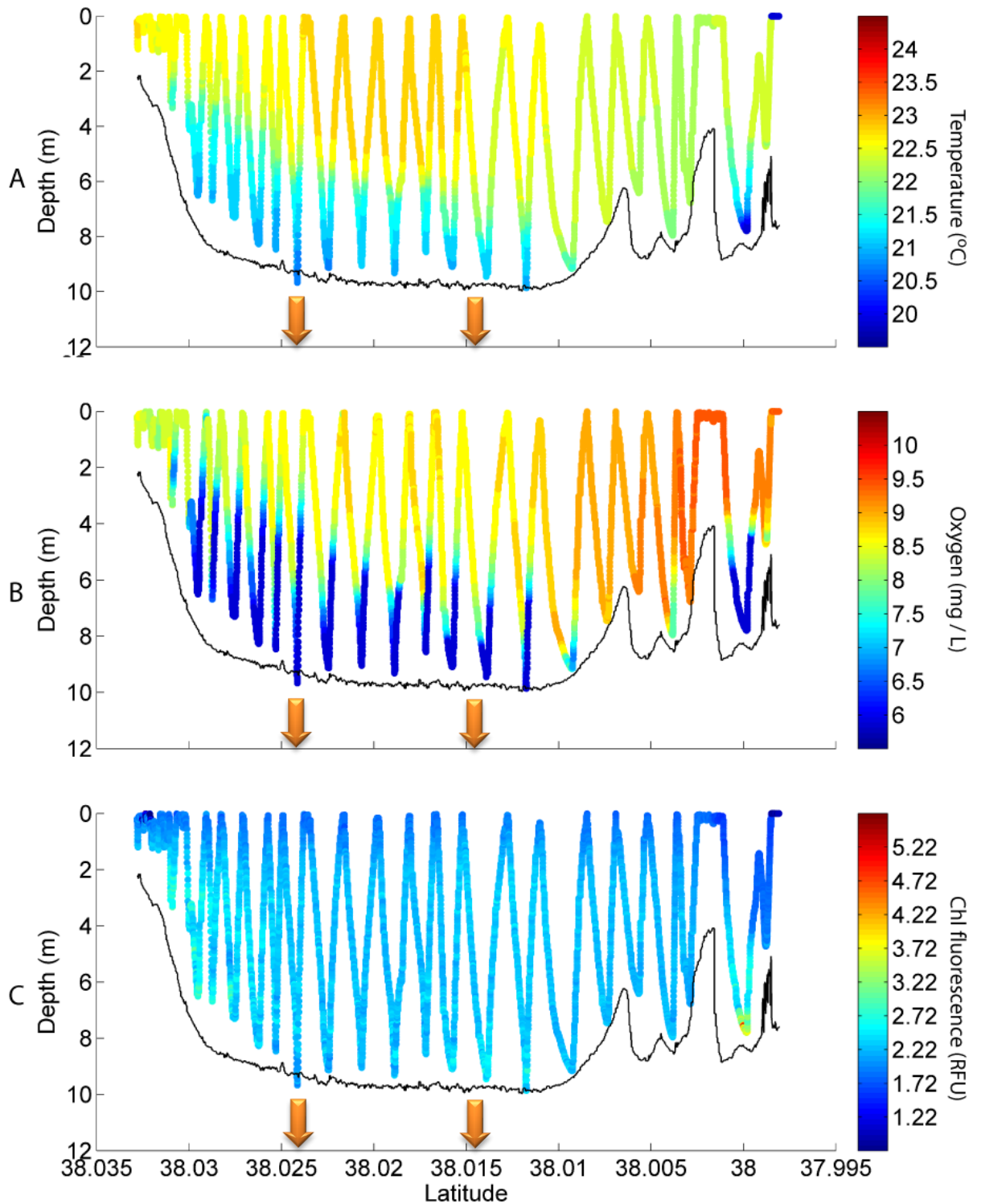


**Figure 17.** Cross section of Lake Rotoehu showing the undulating path of the Bio-Fish device from south (left) to north (right) through the water on 22 February 2013 for A) water temperature, B) dissolved oxygen concentration, and C) chlorophyll fluorescence. The lake was strongly stratified with evidence of oxygen depletion in bottom waters. Note uneven depth of stratification across the transect. Orange arrows denote the location of the mixing devices. The Bio-Fish passed within 100 m of the southern machine, and approximately 350 m from the northern machine (see Figure 2).

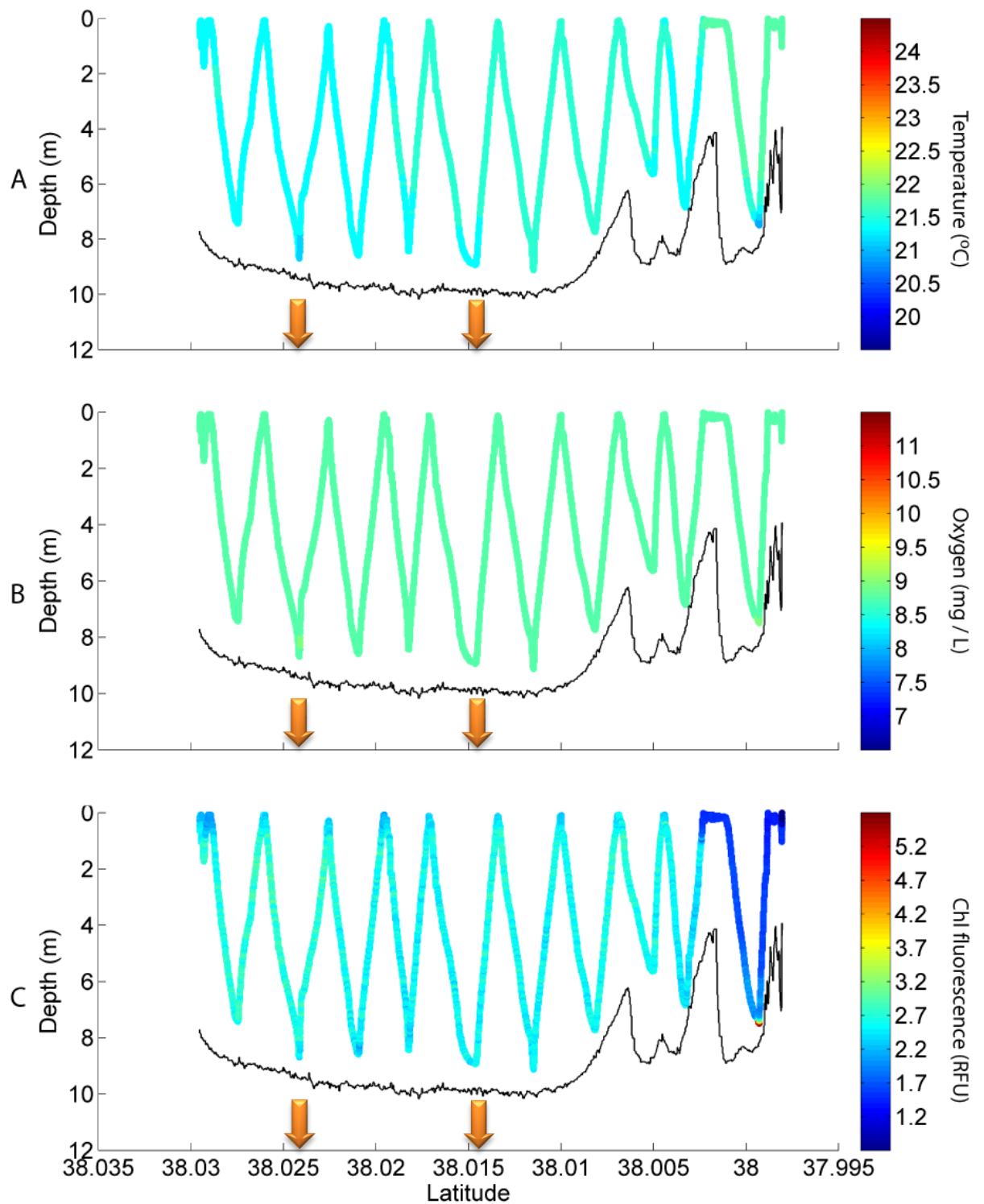


**Figure 18.** Cross-section of Lake Rotoehu showing the undulating path of the Bio-Fish device from south (left) to north (right) through the water on 01 March 2013 for A) water temperature, B) dissolved oxygen concentration and C) chlorophyll fluorescence. Orange arrows denote the location of the mixing devices. The Bio-Fish passed within 100 m of the southern machine, and approximately 350 m of the northern machine (see Figure 2). The mixing devices were turned off on this occasion, although the lake was already fully mixed on this day.

### Dye tracer study

Dye injected into the mixing device northern riser emerged as a clearly visible surface plume, which was diluted as it moved away from the mixing device (Figure 19).



**Figure 19.** Dye plume produced on the lake surface. Mixing device and dye metering equipment on the left with a surface plume visible moving towards the right (north).

Vertical profiles with the Rhodamine probe along the axis of the surface dye plume showed that the majority of the dye sank as it left the mixing device and flowed as a relatively discrete layer along the top of the thermocline, at a depth of about 5 to 8 m for a distance of at least 90 m (Figure 20). The water containing the dye most likely sank due to a density difference between the bottom and surface water, as the colder bottom water emerged out of the top of the mixing device it subsided to find a depth of equal density where it intruded and moved away from the device. This intermediate-depth intrusion indicated that there was sufficient mixing with the warmer surface water to raise its density above that of the bottom water.

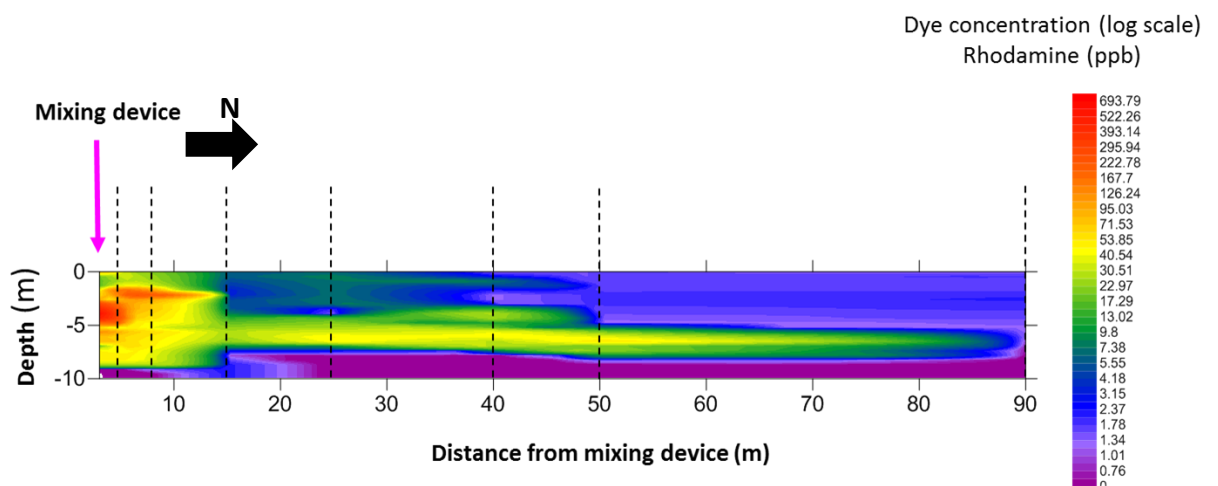


**Figure 20.** Contour plot of the dye plume from the mixing device on 27 February 2013 using Surfer32 by Golden Software. Vertical lines are profiling points. Interpolation between points used triangulation with a ratio of 12:1. The contour plot is a representation of the likely dye flow path based on the available data.

No dye was detected below the thermocline except near the mixing device. In this zone, the dye appeared to be drawn down and recycled through the mixing device by local currents induced by the flow through the mixing device.

### Current measurements

The bottom-tracking-mode ADCP velocities around the mixing device located and defined the positions of each of the three current plumes from the mixing device. The complex pattern indicated that the current plumes gradually dispersed laterally with increasing distance from the mixing device and were difficult to measure beyond about 60-70 m from the mixing device (Figure 21).

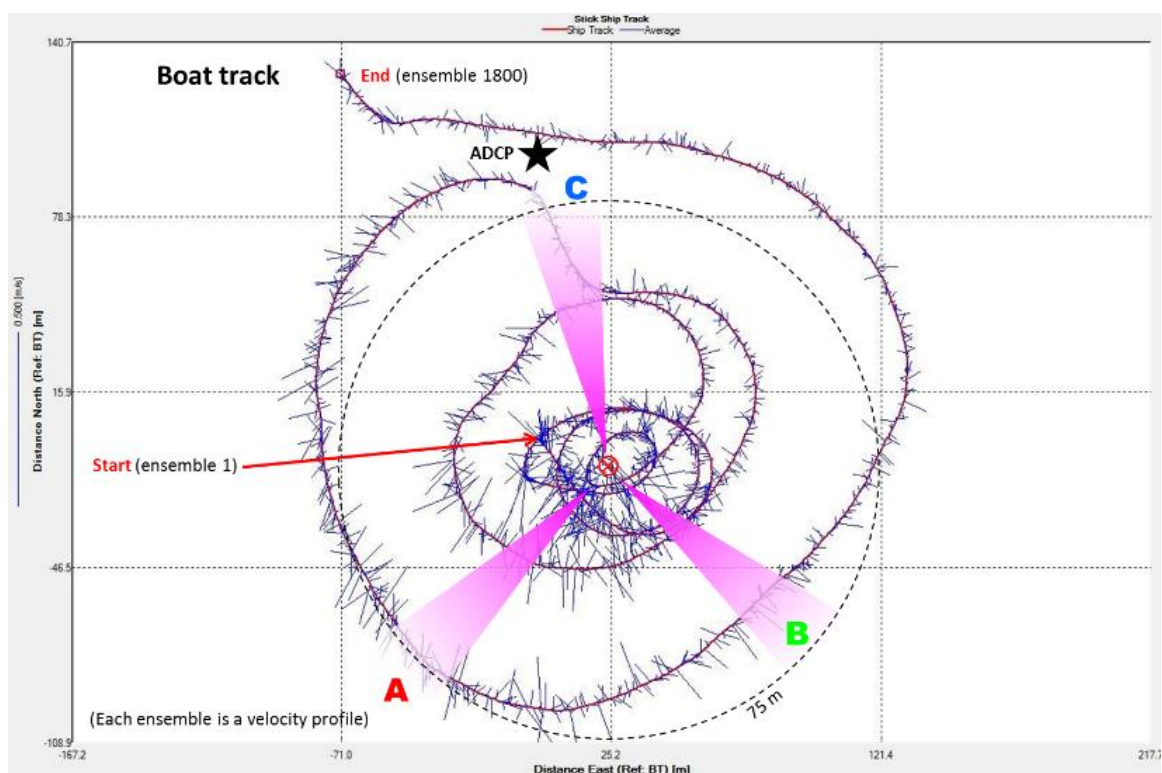


**Figure 21.** Boat path (continuous circular line) of the bottom-tracking ADCP used to locate and define the current flow from each of the arms of the mixing device. The overlay is a stylised representation of the current plume dispersion patterns arbitrarily labelled A, B and C. The Rhodamine dye was injected into arm C.

The ADCP data also indicated a discrete current flow in the mid water column adjacent to the outflow from each of the mixing device arms (Figure 21). The current flow at that depth and distance from the mixing device is consistent with the highest concentration of dye measured by the Rhodamine fluorescence profiling (Figure 19).

The bottom-mounted ADCP recorded current flow velocity and direction at 1-m depth intervals through the water column at the deployment position 100 m from the mixing device. Current velocities were generally low, ranging from  $<1 \text{ cm s}^{-1}$  up to  $25 \text{ cm s}^{-1}$  and averaging around  $5.5 \text{ cm s}^{-1}$  in each depth bin except 1 m below the surface where they averaged  $7.5 \text{ cm s}^{-1}$  (Figure 22). To assess the current flow, the velocity-direction data were converted to vectors and plotted as cumulative sequential distance-travelled graphs (Figure 22). These can be referred to as ‘drifter’ plots and show how a parcel of water moves as it crosses the ADCP. They do not show where the parcel of water went but indicate the direction of the current flow at the ADCP location over the specified time period. The wind data is also converted to a drifter plot but with the direction reversed so that it is towards the direction (not from) to be directly comparable with the current flow direction (Figure 23 A).

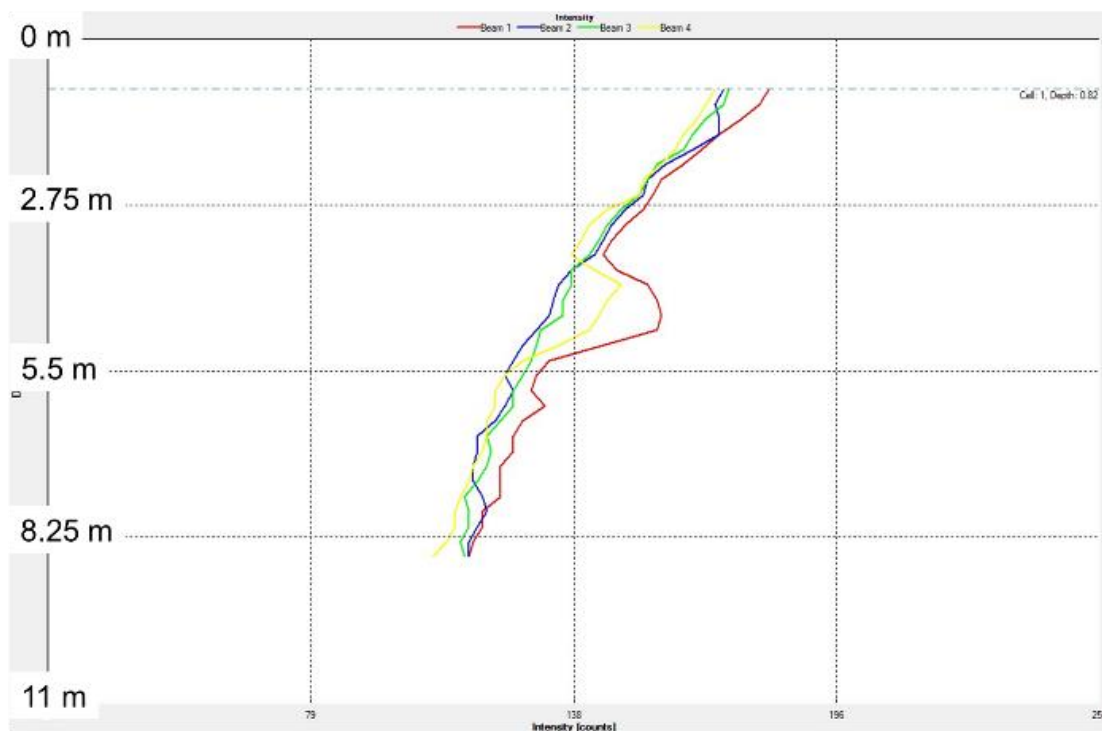


**Figure 22.** Example of the flow pattern from the southern mixing device through the water column depth adjacent to the western arm of the device (Figure 22, arm A) at a distance of 12 m as raw data. The colours represent the 4 acoustic profiler beams. The horizontal axis is “instrument intensity” as counts. The counts are relative to the background intensity slope.



On 26 February, the wind direction was initially erratic before becoming predominantly south-east. The wind direction changed overnight to blow towards the north-west (Figure 23, A). The water flow direction in the upper water column at 3 m depth appeared to be directly coupled with the wind stress on the lake surface and then moved to the south-east on 26 February before following the wind direction change and to the north-west (Figure 23, B). Because the wind data were collected from the meteorological station at Rotorua Airport, 20 km away, the precise time lag for this reversal of water current is uncertain.

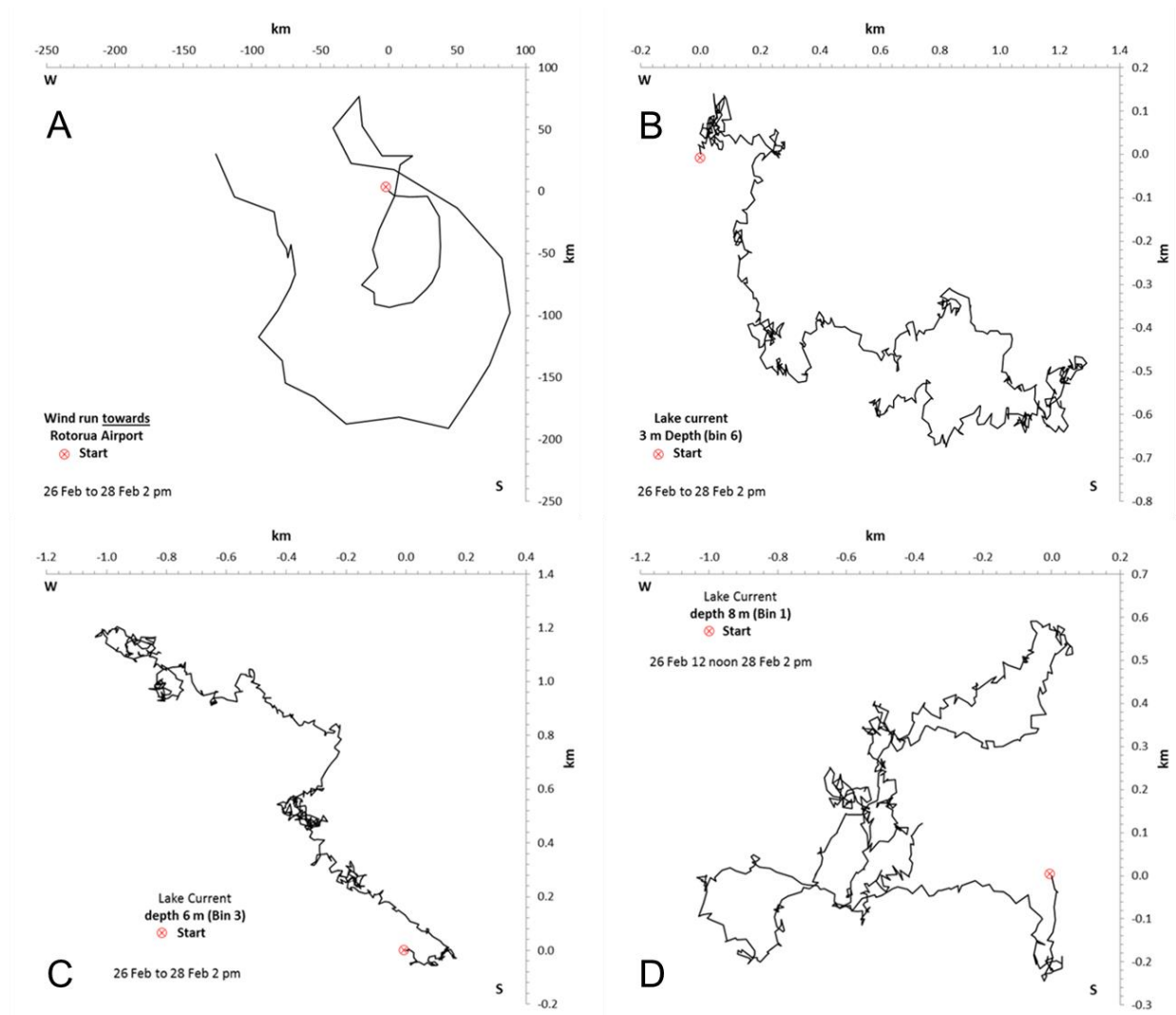


**Figure 23.** Progressive 'drifter' plots of A) wind and water movement at B) 3 m depth, C) 6 m depth and D) 8 m depth from 12:00 noon on 26th February to 2:00 pm on 28th February 2013. (See text for details). The start point for each plot is marked with a ⊗.

In contrast with the water flow direction at 3 m depth, the flow direction at 6 m depth was little affected by the concurrent wind direction. At this depth the water flowed

towards the north-west for the whole period (Figure 23, C). The flow direction at this depth is consistent with the observed plume flow direction from the mixing device (Figure 21) and the depth of the strongest current (Figure 22). Below the thermocline, the water flow directions were not aligned with the wind or the current flow at 6 m depth (Figure 23, D). This indicates that the near bottom water was essentially decoupled from the upper water column due to the presence of the thermocline.

After the mixing device was turned off, the natural lake currents were assumed to have become re-established. Before switching on the device on 18 March, the lake currents at 6 m were moving towards the south-east then south-west and were not coupled with the wind stress on the lake surface (Figure 24). The mixing device was turned on at 10:00 am on 18 March and the current associated with the mixing device at 6 m depth was re-established about 11:00 am on 19 March, indicating a time lag of about 25 h (Figure 24).

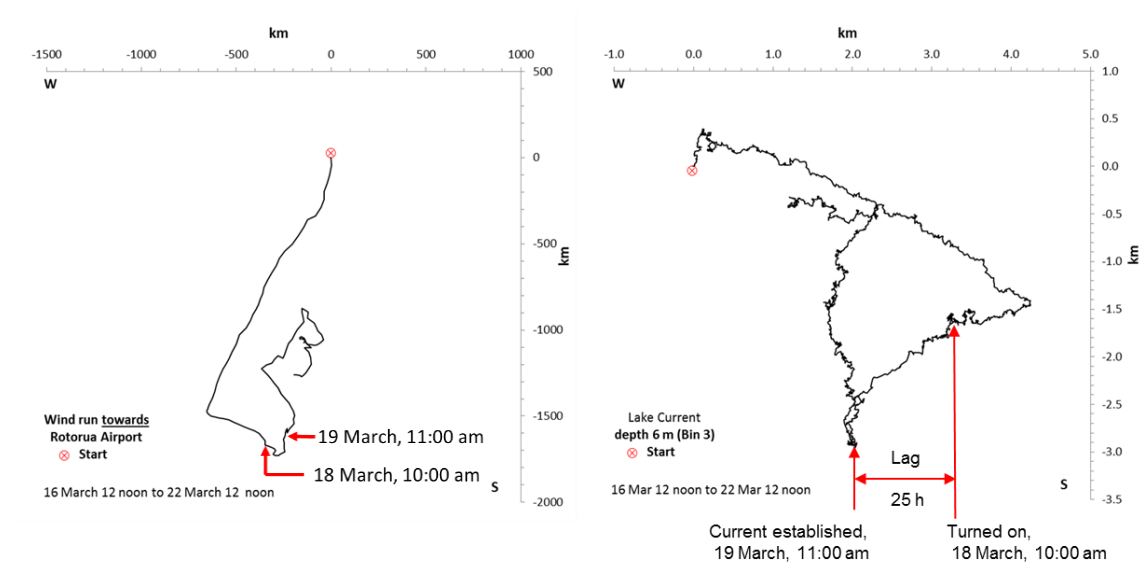


**Figure 24.** Estimating the time lag for the mixing device current to be established after switch on. Date and time of turn of and establishment of the ADCP current 100 m from the mixing device are marked on both plots.

### Nutrient and chlorophyll concentrations

Nutrient concentrations taken from the epilimnion (0.5 m depth) and hypolimnion (9 m depth) near the southern mixing device (Site 1) and at a control site (Site 2) (Figure 2) were taken on 33 occasions from December 2011 to June 2014. The measured epilimnion and hypolimnion concentrations of total nitrogen are shown in Figure 25, total phosphorus in Figure 26, ammonium in Figure 27, nitrate Figure 28 and dissolved phosphorus in Figure 29 during periods of mixing device operation. Paired t-tests were used to look for differences between epilimnion and hypolimnion concentrations and differences between sites. Analysis of total phosphorus, ammonium and nitrate showed no significant difference in concentrations between the epilimnion and hypolimnion or between sites while the mixing devices were in operation. However, increased levels of total nitrogen and decreased levels of dissolved reactive phosphorus were observed in the epilimnion of Site 1 (mixing site) compared to Site 2 (control site). Of note was the large difference in nitrate levels between Site 1 and Site 2 in May and June 2013 in both the epilimnion and hypolimnion (Figure 28). These increased concentrations at Site 1 were present during periods of both mixing device operation and when mixing activity had stopped for the winter season. Also of interest was the decreasing trend in both total and dissolved reactive phosphorus (Figure 25, Figure 29) during the monitoring period.

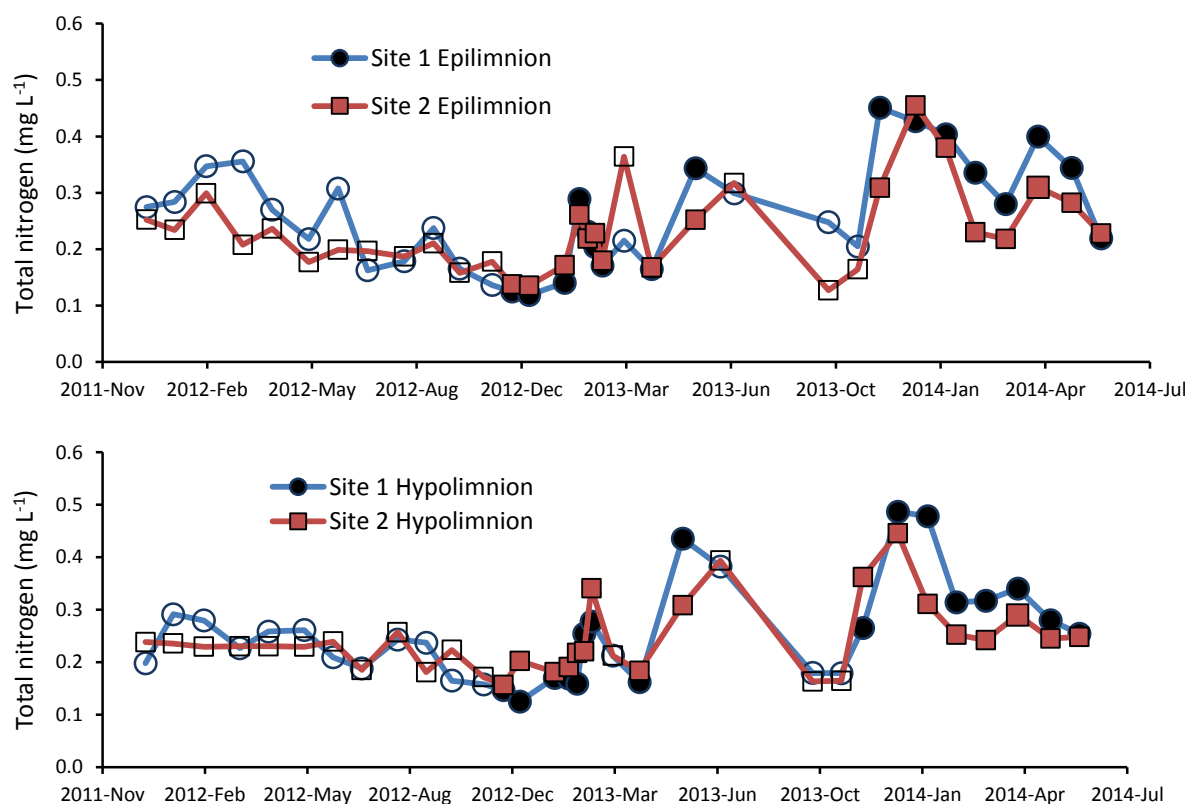


**Figure 25.** Total nitrogen concentrations from the epilimnion (0.5 m) and hypolimnion (9 m) at Site 1 (mixing site) and Site 2 (control site) between 16 December 2011 and 13 June 2014. Open symbols indicate sampling periods when mixing devices were not operating.



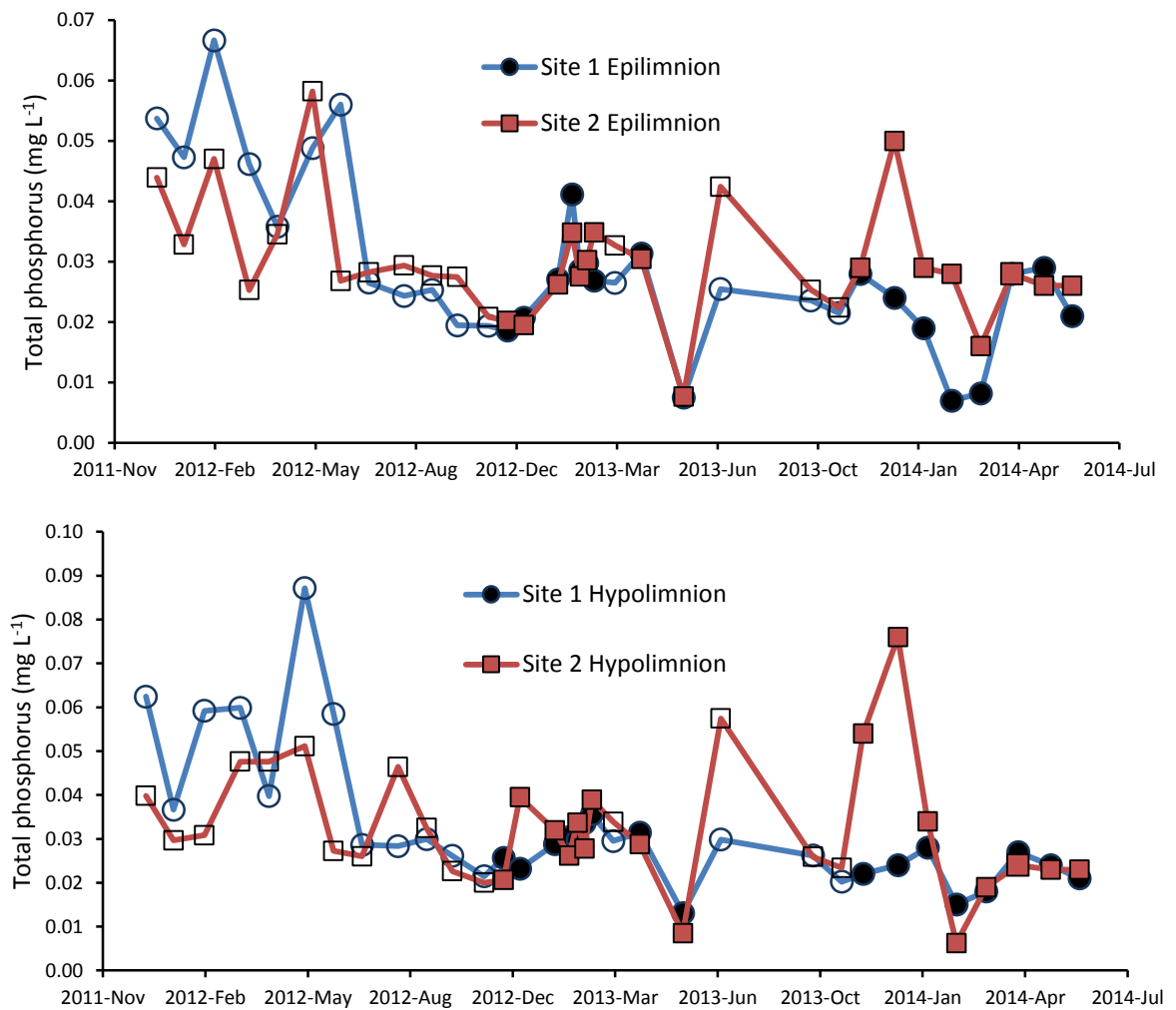


**Figure 26.** Total phosphorus concentrations from the epilimnion (0.5 m) and hypolimnion (9 m) at Site 1 (mixing site) and Site 2 (control site) between 16 December 2011 and 13 June 2014. Open symbols indicate sampling periods when mixing devices were not operating.

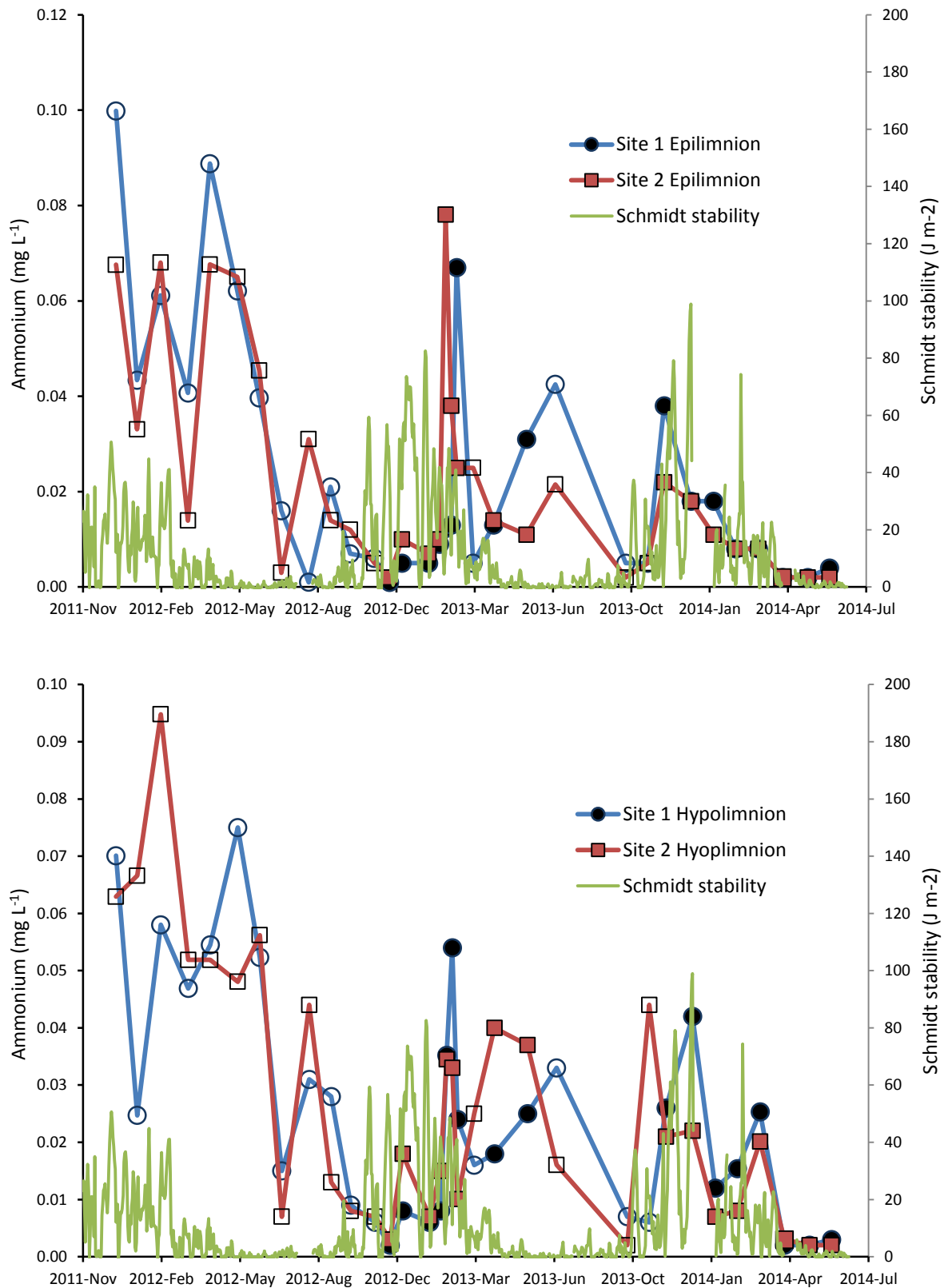


**Figure 27.** Ammonium-nitrogen concentrations from the epilimnion (0.5 m) and hypolimnion (9 m) at Site 1 (mixing site) and Site 2 (control site) between 16 December 2011 and 13 June 2014. Schmidt stability is included for reference to potential lake stratification events. Open symbols indicate sampling periods when mixing devices were not operating.

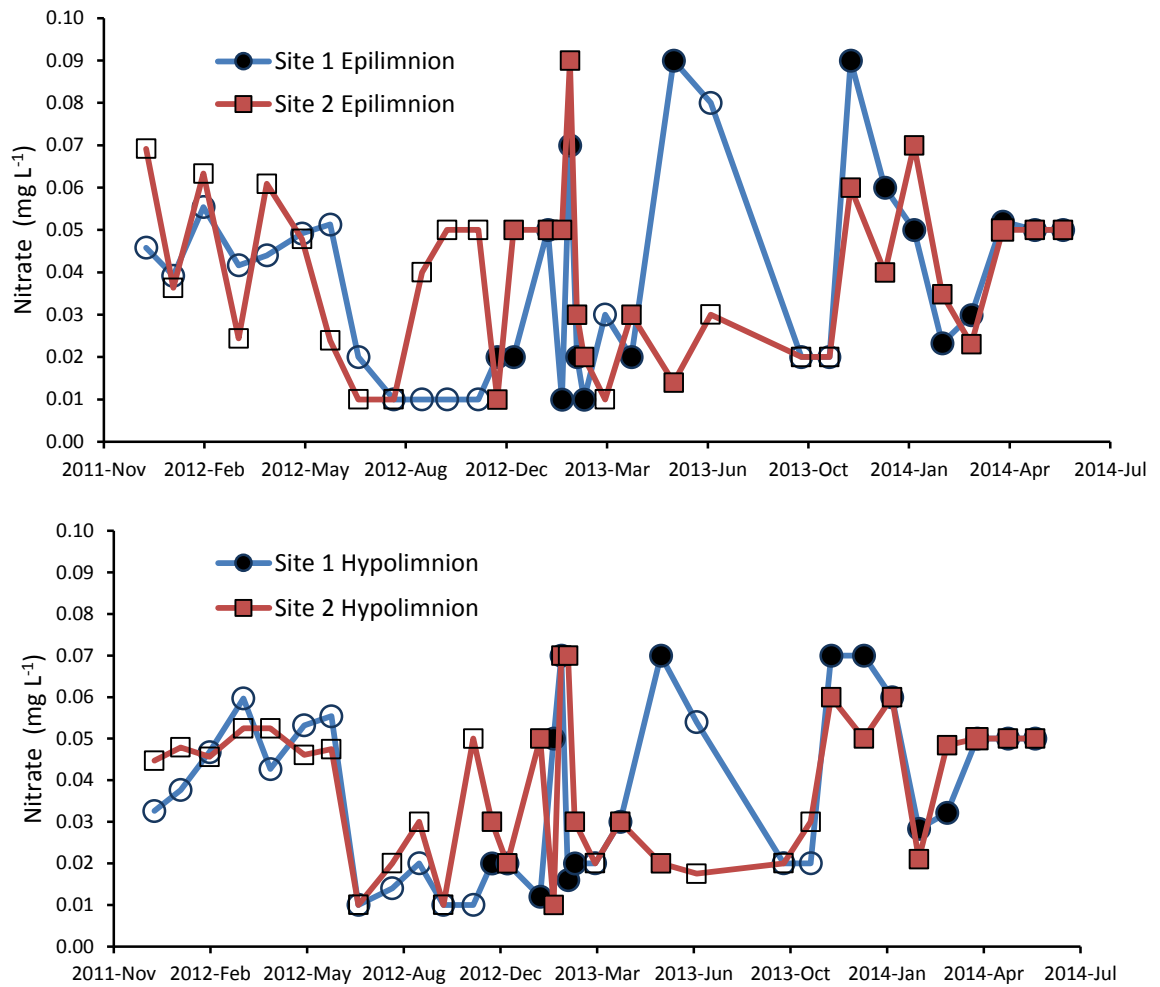


**Figure 28.** Nitrate-nitrogen concentrations from the epilimnion (0.5 m) and hypolimnion (9 m) at Site 1 (mixing site) and Site 2 (control site) between 16 December 2011 and 13 June 2014. Open symbols indicate sampling periods when mixing devices were not operating.

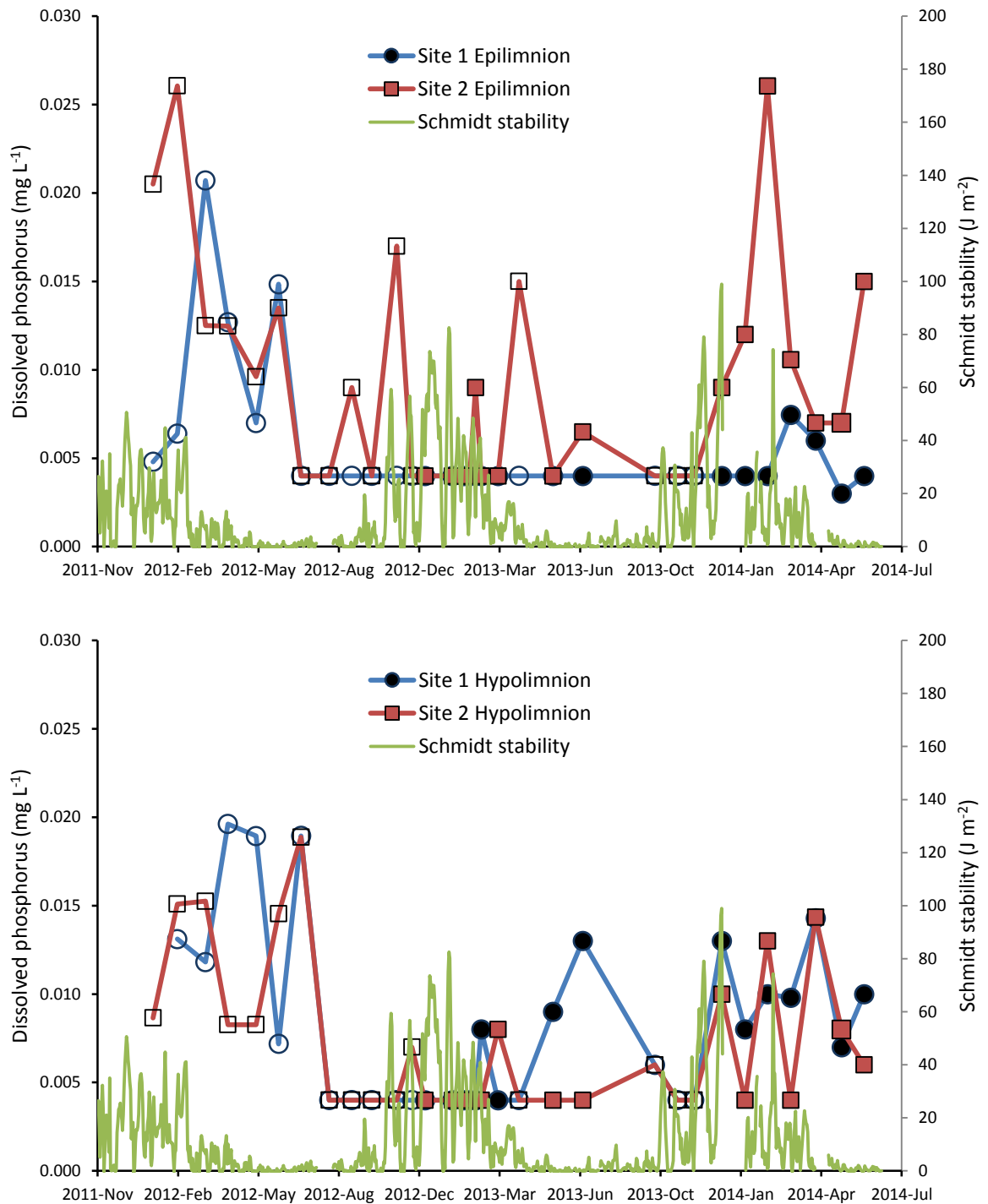


**Figure 29.** Dissolved reactive phosphorus concentrations from the epilimnion (0.5 m) and hypolimnion (9 m) at Site 1 (mixing site) and Site 2 between 16 December 2011 and 13 June 2014. Schmidt stability is included for reference to potential lake stratification events. Open symbols indicate sampling periods when mixing devices were not operating. Note: Dissolved reactive phosphorus concentration detection limit (0.004 mg L<sup>-1</sup>).

Chlorophyll *a* integrated samples (BoPRC) show a seasonal cycle with elevated chlorophyll from autumn through summer. Visual inspection of the time series hints at a decrease over the four-year period (Figure 30), primarily driven by lower summertime chlorophyll levels.

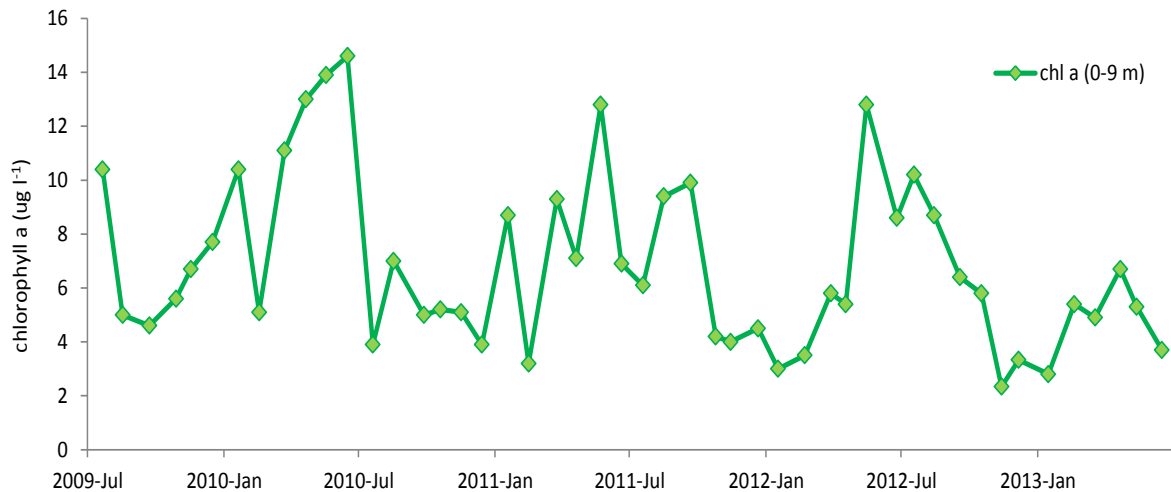


**Figure 30.** Chlorophyll *a* monitoring data from BoPRC, 2009 to 2013.

Chlorophyll *a* samples (UoW) followed a similar pattern at sites 1 and 2 over the 2011 to 2014 monitoring period and in epilimnion (0.5 m) and hypolimnion (9 m) samples. At both sites concentrations peaked in August 2012, and were highly variable during the summer of 2013 (Figure 31). It is notable that despite the observed increased intensity and duration of stratification in summer 2012/13, chlorophyll *a* concentrations were low compared with the previous, more weakly stratified summer (2011/12). Chlorophyll *a* levels were lower and exhibited less variability during the summer of 2013/14 compared with the previous summer. There was no difference in chlorophyll *a* levels between Sites 1 and 2, between the epilimnion and hypolimnion, or when the mixing devices were operating ( $P > 0.05$ ).

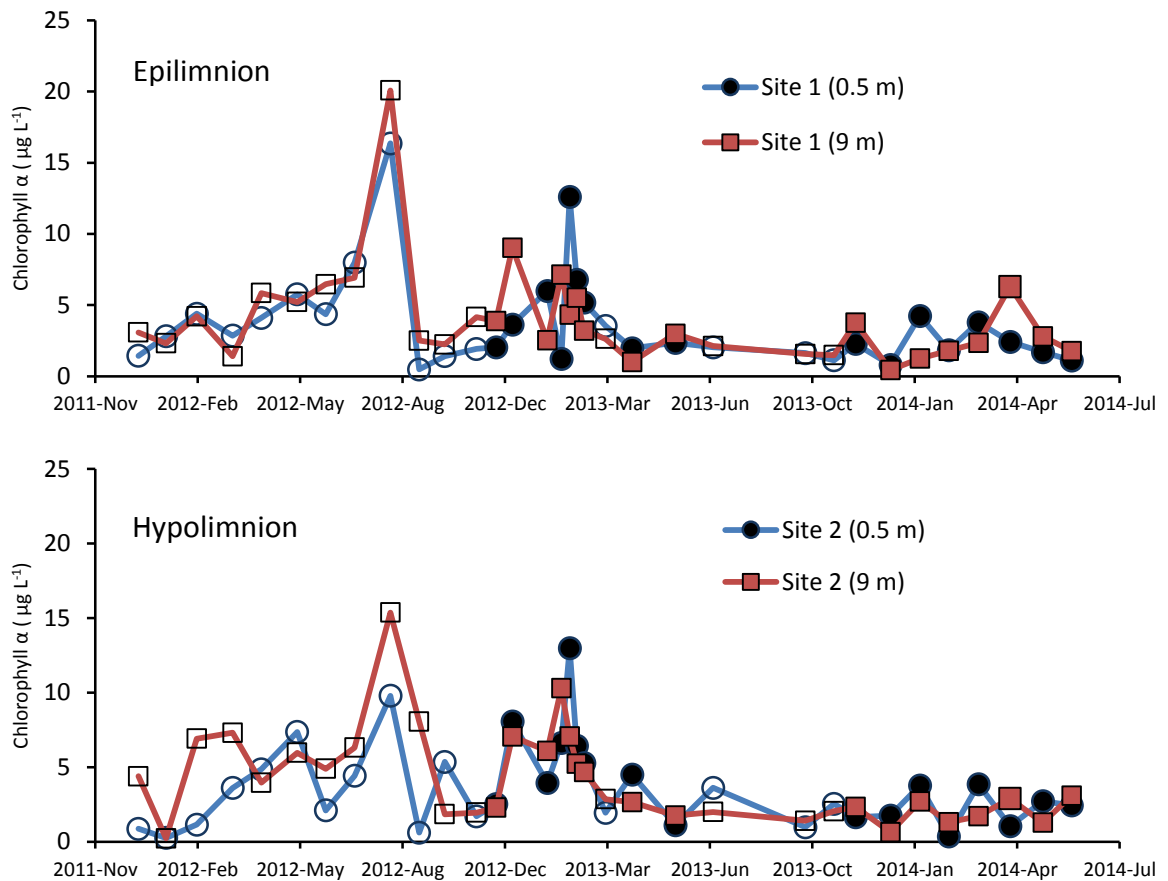


**Figure 31.** Chlorophyll  $a$  at Site 1 (mixing site) and Site 2 (control site) in the epilimnion (0.5 m) and hypolimnion (9 m) between 16 December 2011 and 13 June 2014. Open symbols indicate sampling periods when mixing devices were not operating.

### Plankton communities

Phytoplankton communities were strongly influenced by lake stability. Cyanobacteria abundance increasingly dominated the lake following extended periods of thermal stratification in summer-autumn (Figure 32 and Figure 33). Chlorophytes (green algae) dominated during the 2012 winter-spring months; however, phytoplankton community composition was not consistent between years, due to an extended period of cyanobacteria dominance through winter and early spring of 2013. Relative abundance of diatoms increased during spring and early summer before giving way to increasing cyanobacterial abundance. Relative abundance of cryptophytes was generally below 10% of the phytoplankton cell count, but a notable increase to 20% of the population was observed at Site 1 (mixing site) in May 2014 (Figure 32) driven by higher than normal *Chroomonas* sp. numbers (160 cells  $\text{mL}^{-1}$  c.f. mean 38 cells  $\text{mL}^{-1}$  Site 1 epilimnion) and falling cyanobacteria abundance. Dinoflagellata, euglenophyta and crysophyta collectively comprised <5% of the phytoplankton population and were excluded from further analysis.

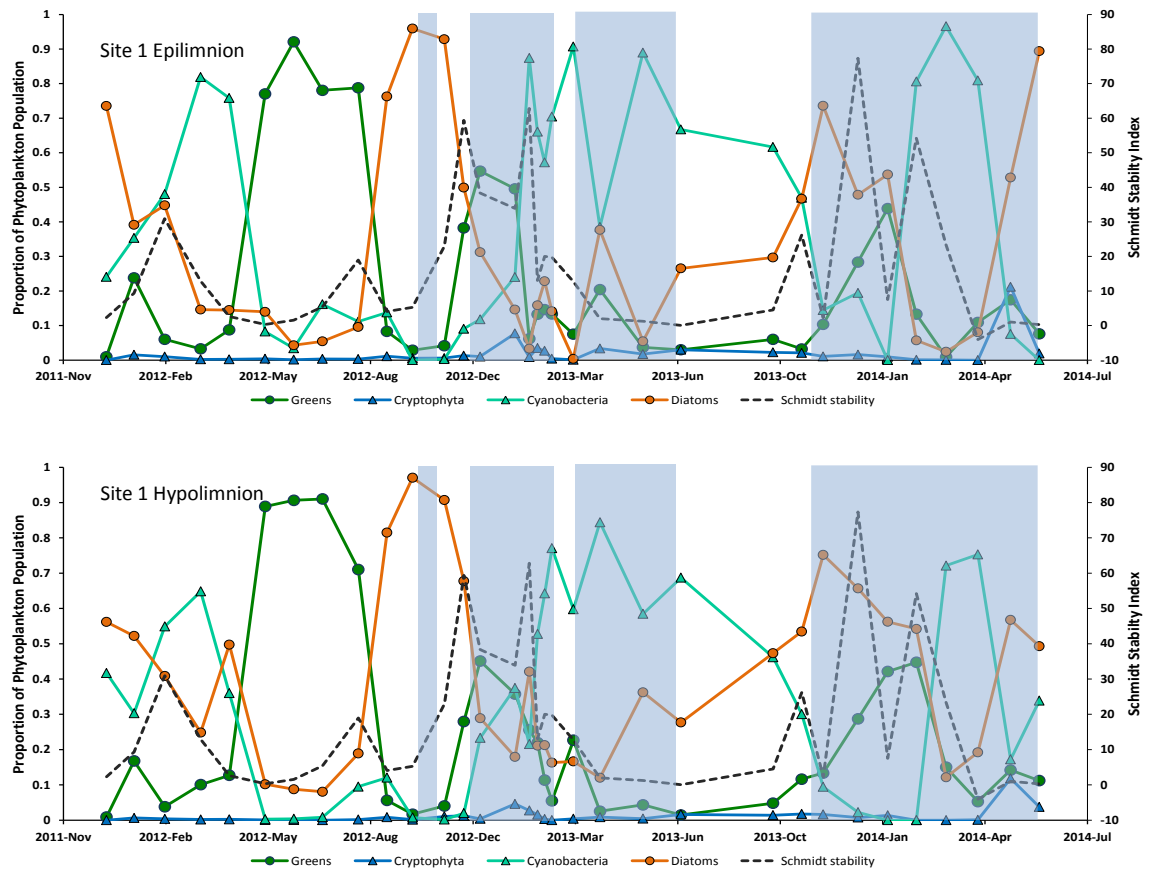


**Figure 32.** Relative cell abundance of Site 1 (mixing site) phytoplankton taxonomic groups from the epilimnion (0.5 m) and hypolimnion (9 m) between 16 December 2011 and 13 June 2014. Dashed line indicates Schmidt stability calculated from CTD temperature data taken at time of sampling. Shaded sections indicate periods when mixing devices were in operation. Note that dinoflagellata, euglenophyta and chrysophyta have been omitted due to low abundance.

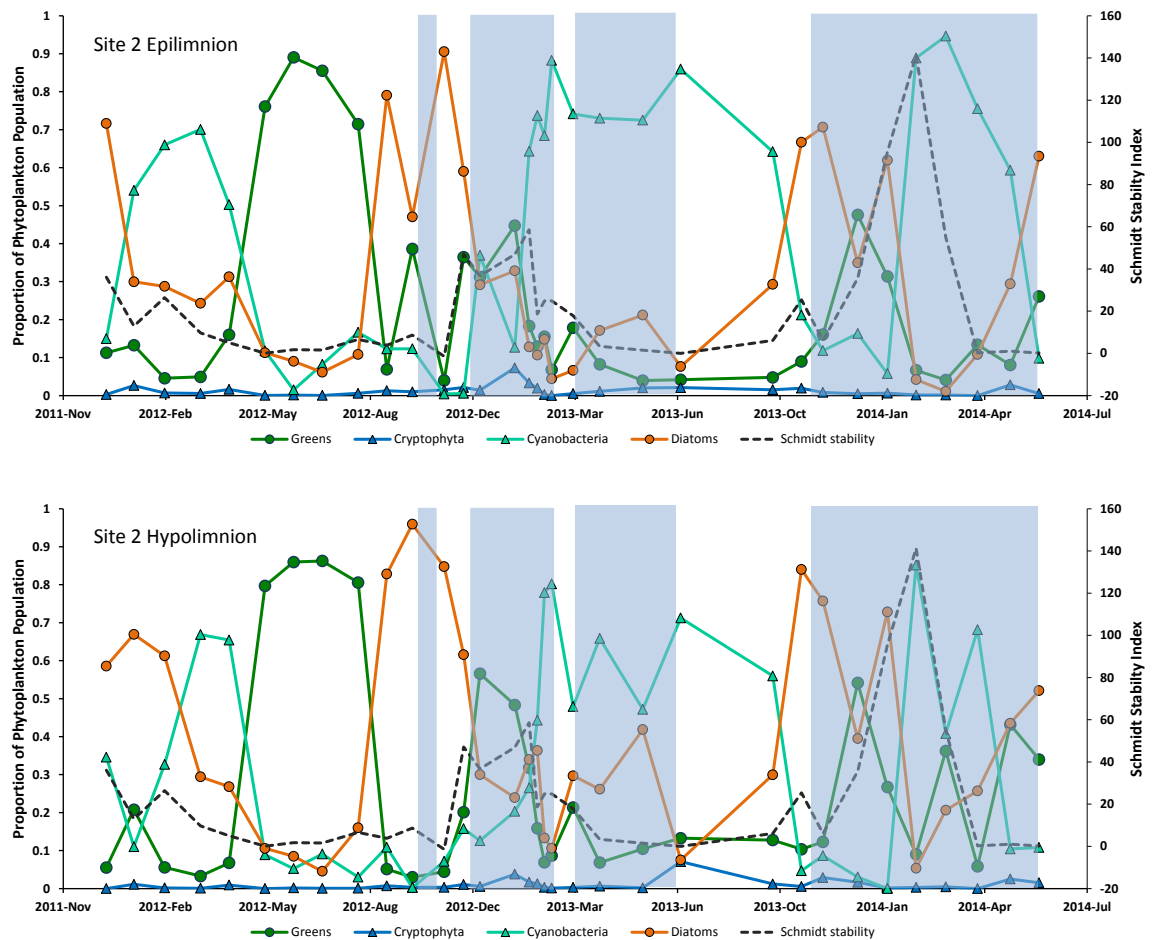


**Figure 33.** Relative cell abundance of Site 2(control site) phytoplankton taxonomic groups from the epilimnion (0.5 m) and hypolimnion (9 m) between 16 December 2011 and 13 June 2014. Dashed line indicates Schmidt stability calculated from CTD temperature data taken at time of sampling. Shaded sections indicate periods when mixing devices were in operation. Note that dinoflagellata, euglenophyta and chrysophyta have been omitted due to low abundance.

Increases in cyanobacteria relative abundance were generally driven by *Anabaena* sp., with a maximum abundance of 7950 cells mL<sup>-1</sup> observed on 31 January 2013 from the mixing site (Site 1) epilimnion. Seasonal increases in diatom abundance varied between years with *Asterionella* sp. and *Aulacoseria* sp. abundant in the spring of 2012 and *Fragilaria* sp. in 2013. Increased group relative abundance in June 2014 was due in part to decreases in cyanobacterial and chlorophyte abundance and a moderate increase in *Aulacoseria* sp. total abundance. Chlorophyte dominance was generally driven by two factors: increasing abundance of *Oocystis* sp. and decreasing abundance of diatoms and cyanobacteria. Peak *Oocystis* sp. absolute abundance occurred in the epilimnion of Site 1 on 14 December 2012 at 1215 cells mL<sup>-1</sup>. Total phytoplankton abundance ranged from 675 to 16607 cells mL<sup>-1</sup> with a mean of 4489 cells mL<sup>-1</sup> for all samples. Peak total abundance occurred during the winter (June-August) of 2012 (Figure 34) and a secondary bloom was present in March and April 2014.



The large peak in chlorophyll *a* observed in August 2012 (Figure 31) was due to atypical concurrent high abundances of cyanobacteria (primarily *Anabaena* sp.), diatoms (*Asterionella* sp. and *Aulacoseira* sp.) and the chlorophyte species *Dictyosphaerium* sp. Mean phytoplankton abundance at this time was 11915 cells mL<sup>-1</sup>, more than double the mean of 4489 cells mL<sup>-1</sup> for all samples.

Total abundance analysis of the main (>5% community abundance) phytoplankton taxonomic groups (chlorophyta, diatoms, cryptophyta and cyanobacteria) found chlorophytes to be significantly (t-test;  $P=0.03$ ) less abundant in the mixing site (Site 1) hypolimnion compared to the control site (Site 2) hypolimnion when the mixing devices were operating (Table 2). Tests for differences between epilimnion and hypolimnion of Site 1 found higher abundance in chlorophyta ( $P=0.03$ ) and cryptophyta (t-test;  $P=0.02$ ) when mixing devices were operating and higher epilimnion cryptophyta abundance when the devices were off (t-test;  $P=0.02$ ). There were also significant differences in cryptophyta total abundance between the epilimnion and hypolimnion at Site 2 when the mixing devices were switched off. Also of interest was the higher cyanobacteria total abundance in the Site 2 epilimnion compared to the Site 2 hypolimnion (t-test;  $P < 0.01$ ). No other significant differences in total abundance were present, however there was generally greater homogeneity in phytoplankton abundance between depths at Site 1 when the device was operating compared to Site 2 and when the device was shut off (Table 2).

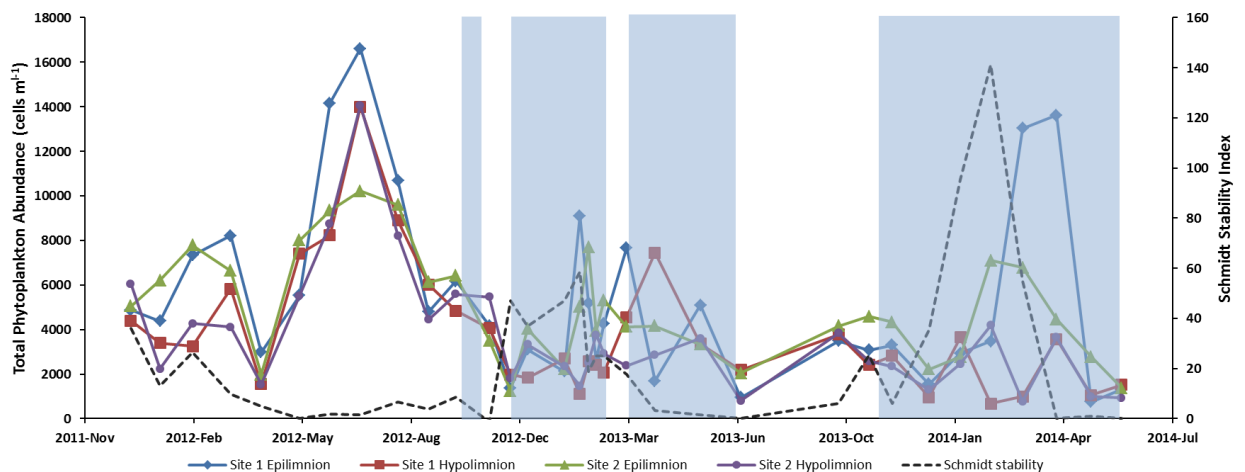


**Figure 34.** Total phytoplankton cell abundance in the epilimnion (0.5 m) and hypolimnion (9 m) of Site 1 (mixing site) and Site 2 between 16 December 2011 and 13 June 2014. Dashed line indicates Schmidt stability calculated from CTD temperature data taken at time of sampling. Shaded sections indicate periods when mixing devices were in operation.

**Table 2.** Analysis of Lake Rotoehu phytoplankton taxonomic group abundance. Data were allocated to periods when either the mixing devices were operating (ON) or shut down (OFF); Student's t-tests were then conducted between the mixing site (Site 1) and control site (Site 2) and between two depths, the epilimnion (0.5 m) and the hypolimnion (9 m). Means that are significantly different are presented in bold.

Site 1 vs Site 2 Epilimnion	OFF		ON	
	Mean cells mL <sup>-1</sup>	P value	Mean cells mL <sup>-1</sup>	P value
Site 1 Total Chlorophyta	532		441	
Site 2 Total Chlorophyta	789	0.10	536	0.21
Site 1 Total Diatoms	1064		617	
Site 2 Total Diatoms	1243	0.33	648	0.77
Site 1 Total Cryptophyta	24		32	
Site 2 Total Cryptophyta	33	0.32	22	0.15
Site 1 Total Cyanobacteria	661		590	
Site 2 Total Cyanobacteria	766	0.76	1499	0.07

Site 1 vs Site 2 Hypolimnion				
Site 1 Total Chlorophyta	491		<b>297</b>	
Site 2 Total Chlorophyta	545	0.62	<b>415</b>	<b>0.03</b>
Site 1 Total Diatoms	1481		618	
Site 2 Total Diatoms	1215	0.22	622	0.94
Site 1 Total Cryptophyta	11		14	
Site 2 Total Cryptophyta	11	0.78	13	0.85
Site 1 Total Cyanobacteria	355		300	
Site 2 Total Cyanobacteria	528	0.36	401	0.61

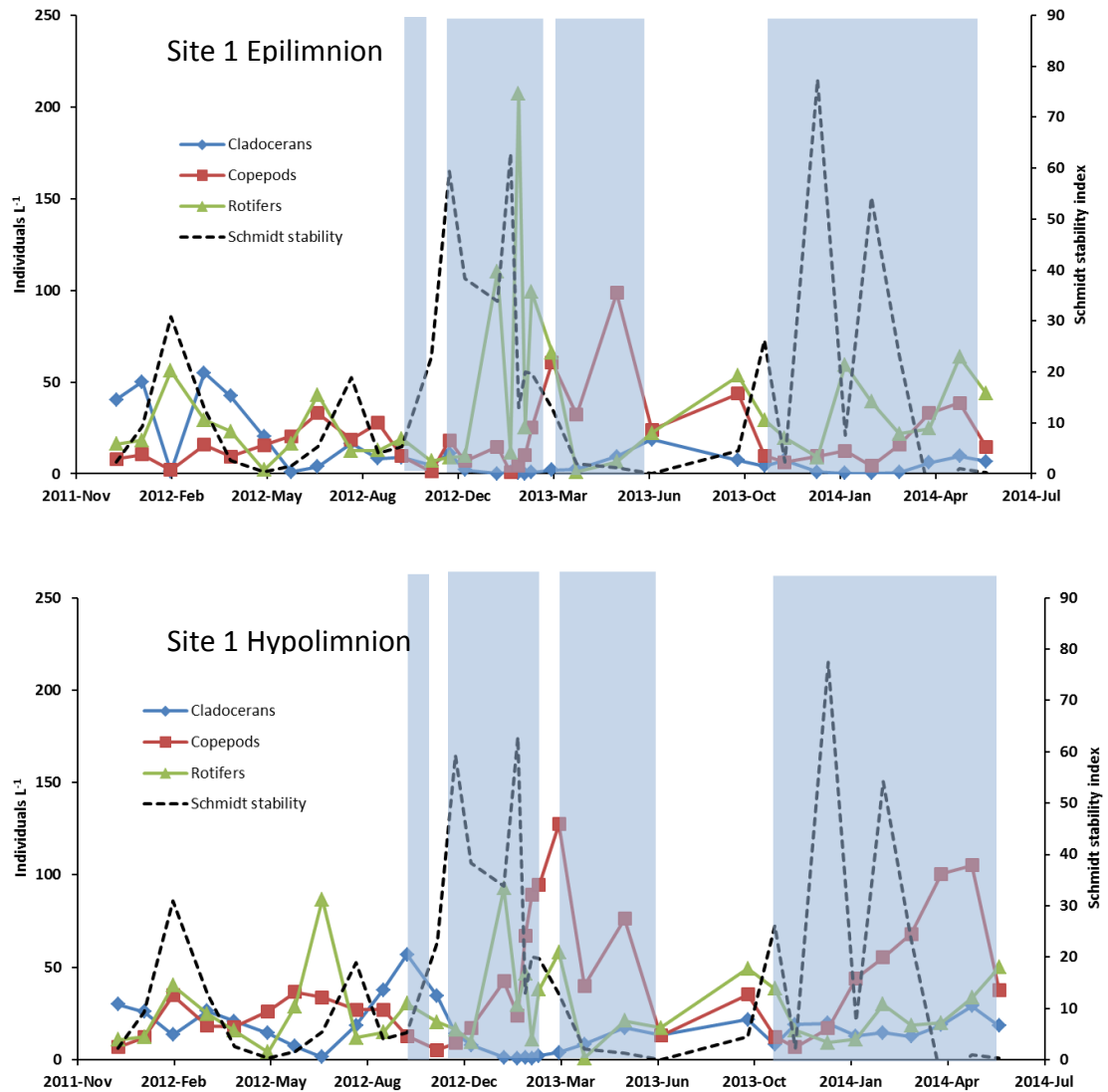
Site 1 Epilimnion vs Hypolimnion				
Epi Total Chlorophyta	532		<b>441</b>	
Hypo Total Chlorophyta	491	0.58	<b>297</b>	<b>0.03</b>
Epi Total Diatoms	1064		617	
Hypo Total Diatoms	1481	0.14	618	0.99
Epi Total Cryptophyta	<b>24</b>		<b>32</b>	
Hypo Total Cryptophyta	<b>11</b>	<b>0.02</b>	<b>14</b>	<b>0.02</b>
Epi Total Cyanobacteria	661		590	
Hypo Total Cyanobacteria	355	0.12	300	0.38

Site 2 Epilimnion vs Hypolimnion				
Epi Total Chlorophyta	789		536	
Hypo Total Chlorophyta	545	0.07	415	0.10
Epi Total Diatoms	1243		648	
Hypo Total Diatoms	1215	0.84	622	0.72
Epi Total Cryptophyta	<b>33</b>		22	
Hypo Total Cryptophyta	<b>11</b>	<b>&lt;0.01</b>	13	0.08
Epi Total Cyanobacteria	766		<b>1499</b>	
Hypo Total Cyanobacteria	528	0.44	<b>401</b>	<b>&lt;0.01</b>

Zooplankton taxonomic group (rotifers, cladocerans and copepods) total numerical abundance was plotted over time for each site and sampling depth (Figure 35 and Figure 36). Rotifers were more abundant in the epilimnion of both sites with peak abundance occurring in the January-February period of 2013. Rotifer abundance appeared to be highly variable, not only between seasons but also within seasons. For example, large changes in rotifer abundance were observed in the January-March 2013 period at both sampling sites, with rotifer abundance at Site 1 (mixing site) ranging from 0.6 individuals  $L^{-1}$  on 31 January 2013 to 207 individuals  $L^{-1}$  on 8 February 2013 before decreasing again to 25.3 individuals  $L^{-1}$  on 15 February. These changes did not appear to be correlated with lake stability or mixing device operation. Copepod abundance was less variable, although peaks of 100–150 individuals  $L^{-1}$  did occur in the autumn (March–May) of 2013 and 2014; this was particularly evident in the hypolimnion samples from both sites. Increases in copepod abundance appeared to be moderately correlated with decreasing lake stability. Cladoceran abundance exhibited the least variability, with peaks occurring during the late winter–spring when there were associated increases in diatom abundance (Figure 35 and Figure 36.)

Analysis of zooplankton taxonomic group abundance in relation to mixing device operation found no significant differences in zooplankton abundance between mixing (Site 1) and control (Site 2) sites in the epilimnion, both when the devices were operating and when shut off (t-tests;  $P>0.05$ ) (Table 3). Rotifer abundance was higher in the Site 1 hypolimnion (mean 22 individuals  $L^{-1}$ ) compared to the Site 2 hypolimnion (mean 14 individuals  $L^{-1}$ ) when the devices were off (t-test;  $P<0.01$ ); however, no other differences were observed between Site 1 and Site 2 hypolimnion zooplankton abundance (Table 3). Significantly higher abundances (t-test;  $P>0.05$ ) of cladocerans and copepods were present in the hypolimnion compared to epilimnion at both sites when the mixing devices were operating (Table 3). Although, this pattern of higher hypolimnion cladoceran and copepod abundances was repeated when the mixing devices were not operating, only the Site 2 cladoceran group was significantly higher (t-test;  $P=0.04$ ). In contrast, rotifer abundances were comparatively even between the epilimnion and hypolimnion irrespective of site and mixing device status (Table 3).



**Figure 35.** Lake Rotoehu zooplankton group abundance for Site 1 (mixing site) epilimnion (0.5 m) and hypolimnion (9 m) between 16 December 2011 and 13 June 2014. Dash line indicates Schmidt stability calculated from CTD temperature data taken at time of sampling. Shaded sections indicate periods when mixing devices were in operation.

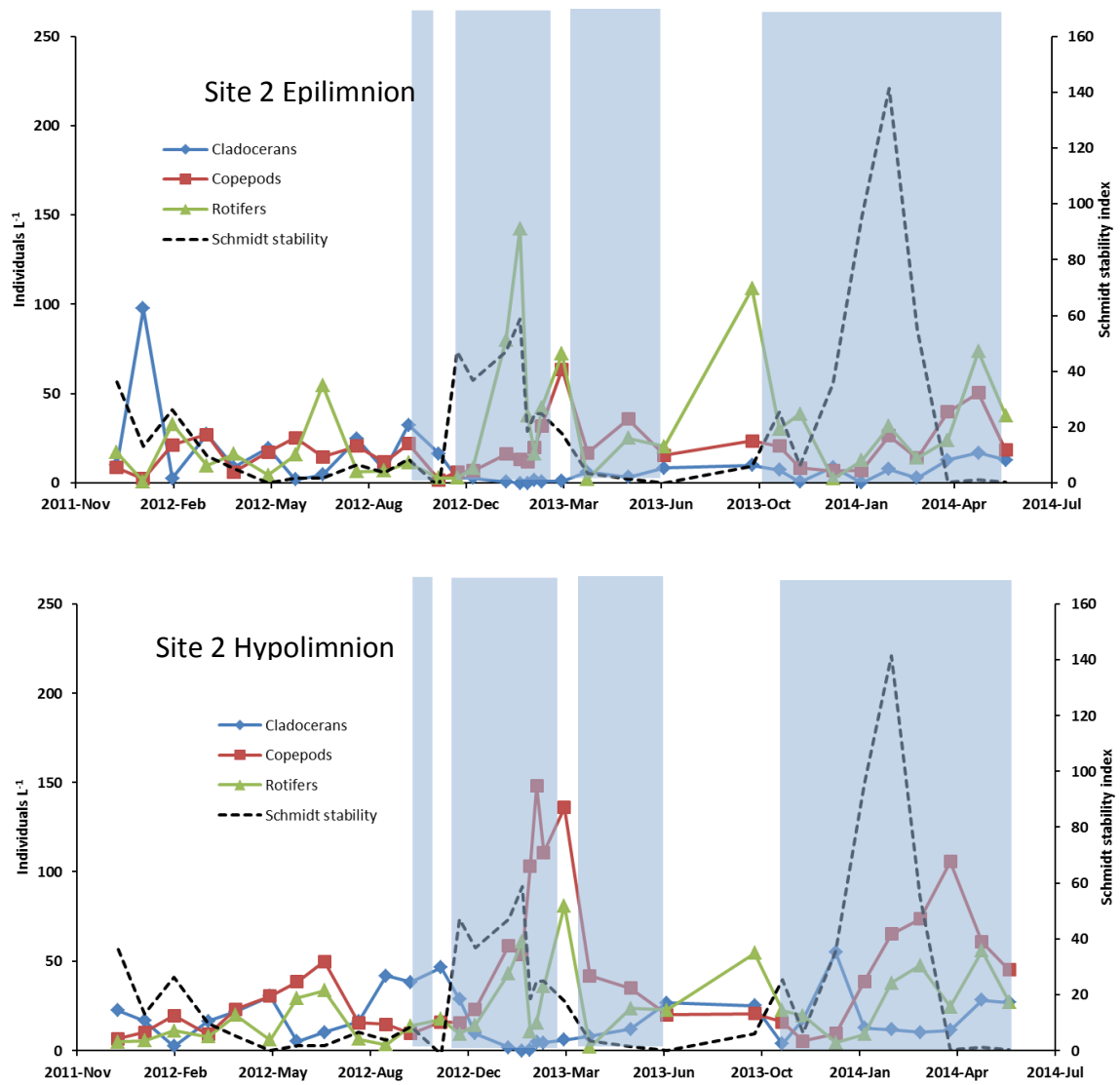


**Figure 36.** Lake Rotoehu zooplankton group abundance for Site 2 (control site) epilimnion (0.5 m) and hypolimnion (9 m) between 16 December 2011 and 13 June 2014. Dash line indicates Schmidt stability calculated from CTD temperature data taken at time of sampling. Shaded sections indicate periods when mixing devices were in operation.

**Table 3.** Analysis of Lake Rotoehu zooplankton taxonomic group abundance. Data were allocated to periods when either the mixing devices were operating (ON) or shut down (OFF); Student's t-tests were then conducted between the mixing site (Site 1) and control site (Site 2) and between two depths, the epilimnion (0.5 m) and the hypolimnion (9 m). Means that are significantly different are presented in bold.

Site 1 vs Site 2 Epilimnion	OFF		ON	
	Mean Individuals L <sup>-1</sup>	P value	Mean Individuals L <sup>-1</sup>	P value
Site 1 Total Cladocerans	10		2	
Site 2 Total Cladocerans	10	0.80	3	0.28
Site 1 Total Copepods	14		13	
Site 2 Total Copepods	14	0.85	17	0.24
Site 1 Total Rotifers	20		23	
Site 2 Total Rotifers	13	0.06	23	0.98
Site 1 vs Site 2 Hypolimnion				
Site 1 Total Cladocerans	16		8	
Site 2 Total Cladocerans	16	0.91	8	0.65
Site 1 Total Copepods	20		45	
Site 2 Total Copepods	19	0.86	47	0.64
Site 1 Total Rotifers	<b>22</b>		20	
Site 2 Total Rotifers	<b>14</b>	<b>&lt;0.01</b>	20	0.86
Site 1 Epilimnion vs Hypolimnion				
Epi Total Cladocerans	10		<b>2</b>	
Hypo Total Cladocerans	16	0.09	<b>8</b>	<b>&lt;0.001</b>
Epi Total Copepods	14		<b>13</b>	
Hypo Total Copepods	20	0.08	<b>45</b>	<b>&lt;0.001</b>
Epi Total Rotifers	20		23	
Hypo Total Rotifers	22	0.26	20	0.58
Site 2 Epilimnion vs Hypolimnion				
Epi Total Cladocerans	<b>10</b>		<b>3</b>	
Hypo Total Cladocerans	<b>16</b>	<b>0.04</b>	<b>8</b>	<b>&lt;0.001</b>
Epi Total Copepods	14		<b>17</b>	
Hypo Total Copepods	19	0.09	<b>47</b>	<b>&lt;0.001</b>
Epi Total Rotifers	13		23	
Hypo Total Rotifers	14	0.77	20	0.35

A Bray-Curtis similarity index was used to compare the degree of similarity in the plankton (i.e., zooplankton and phytoplankton) community between Site 1 (mixing site) and Site 2 (control) for both the epilimnion (0.5 m) and hypolimnion (9.0 m) depths (Figure 37). The Bray-Curtis similarity index is based on a scale of 0 – 100, therefore, the closer the index to 100, the greater the community similarity. Plankton communities displayed a high level of similarity between sites and depths; the mean Bray-Curtis similarity between Site 1 and Site 2 epilimnion was 75.0, and 75.4 for the hypolimnion. Although the community similarity between the epilimnion samples did decrease noticeably in comparison to the hypolimnion for March and April 2013 period, this appeared to have no clear relationship to mixing device operation (Figure 37).

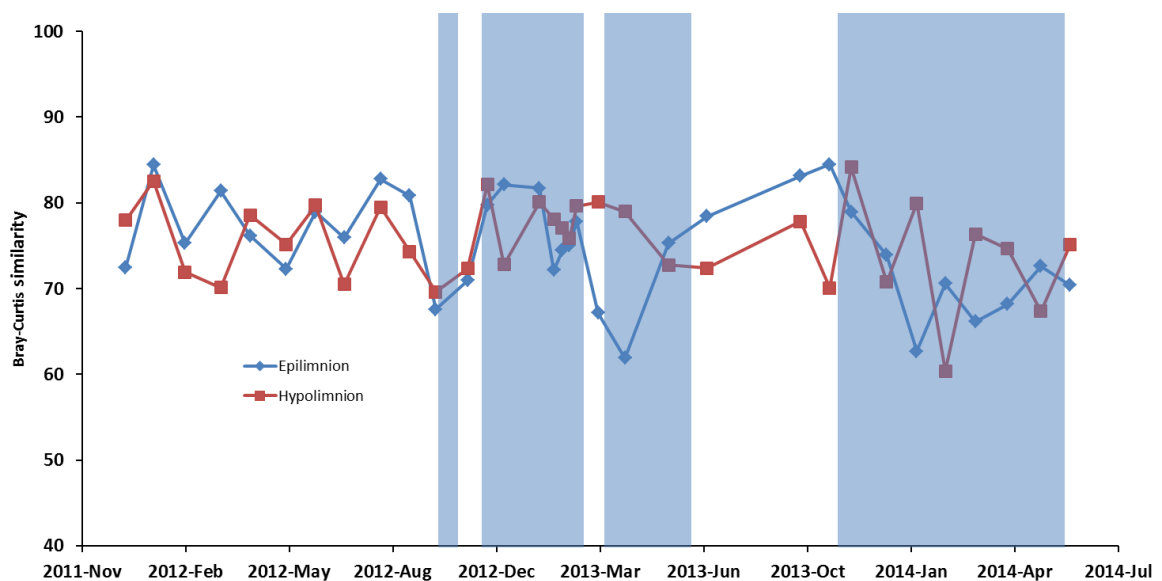


**Figure 37.** Degree of similarity (Bray-Curtis) in plankton community composition between Site 1 (mixing site) and Site 2 (control site) for both the epilimnion (0.5 m) and hypolimnion (9 m) layers in Lake Rotoehu between 16 December 2011 and 13 June 2014. Shaded sections indicate periods when mixing devices were in operation.

Mean Bray-Curtis plankton community similarity between the epilimnion and hypolimnion for Site 1 (mixing site) and Site 2 (control site) was 72.5 and 73.4 respectively. A large decline in community similarity was observed between the Site 1 epilimnion and hypolimnion on 13 February 2014 before returning to a more typical range of values in the following months (Figure 38). This difference appears to be primarily driven by the phytoplankton species *Anabaena* sp. (2802 cells mL<sup>-1</sup>), *Dictyosphaerium* sp. (255 cells mL<sup>-1</sup>), present in the Site 1 epilimnion that were not detected in the hypolimnion, and low levels (<50 cells mL<sup>-1</sup>) of *Cyclotella* sp., *Synedra* sp., *Closterium* sp. and *Coelastrum* sp. observed in the hypolimnion but not in the epilimnion.

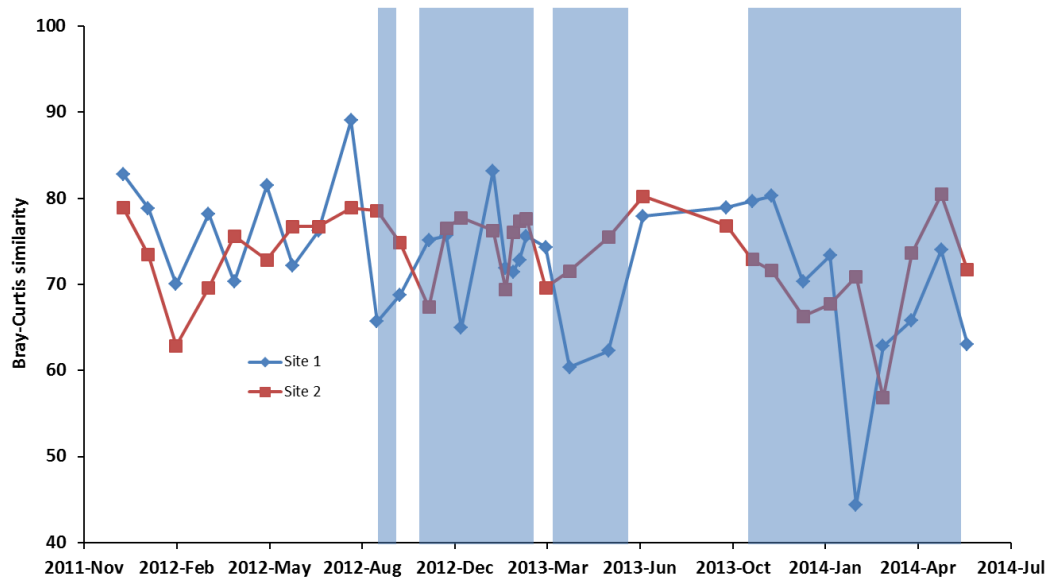


**Figure 38.** Degree of similarity (Bray-Curtis) in plankton community composition between the epilimnion (0.5 m) and hypolimnion (9 m) layers of the Site 1 (mixing site) and Site 2 (control site) locations in Lake Rotoehu between 16 December 2011 and 13 June 2014. Shaded sections indicate periods when mixing devices were in operation.

Plankton species subdivided into phytoplankton and zooplankton communities were assessed for degree of similarity between sites and depths. The phytoplankton community displayed a comparable degree and pattern of similarity to that observed in the plankton community analysis (Figure 37 and Figure 38). The results of the phytoplankton similarity analysis are presented in Appendix 1. The zooplankton community also displayed a comparable degree and pattern of similarity to the whole plankton community analysis. However, an anomalous result was observed for the Site 1 epilimnion on 31 January 2013 (Appendix 1). The zooplankton species present in this sample were similar to those observed at Site 2 on the same date, but abundance of all species was considerably lower at the mixing site (Site 1). This result was confirmed by cross-checking against a duplicate Site 1 zooplankton sample taken on that date.



## Discussion

A multi-faceted monitoring approach has provided considerable insight into the effects of deployment of two artificial water column mixing devices deployed in Lake Rotoehu from November 2012 to June 2014. Water column profiles show that these mixing devices are capable of modifying the thermal structure of the water column in the immediate vicinity of the device, but effects are curtailed rapidly and there is little evidence of any effect at distances greater than about 200 m.

Several factors specific to Lake Rotoehu may have reduced the efficiency of the devices. Macrophytes, principally hornwort (*Ceratophyllum demersum*), are abundant in Rotoehu and frequently form large floating 'rafts' of weed. These were observed to regularly foul the intake of the devices, thus reducing flow rates. Macrophytes may also further reduce the effectiveness of the devices by disrupting horizontal flow near the lake bottom, and interfering with horizontal dispersion near the surface.

Dense, cold water pumped from the hypolimnion had limited entrainment with warm surface waters, and tended to sink rapidly to an intermediate depth close to a weak thermocline. This could explain the localised effects on the lake thermal structure observed during the dye tracer study. Refinement of the device moorings, air flow rates, and protection from weed fouling may improve horizontal dispersion, increase entrainment and lead to more effective mixing of surface and bottom waters. In addition, previous modelling of the mixing devices by UoW found the shallow depth of Rotoehu provides insufficient time for hypolimnetic water entrained in the upward plume to become air-saturated in transit.

The limited spatial extent of destratification is consistent with predictions from mathematical modelling carried out by UoW before the deployment of the devices in Rotoehu (unpublished data). Although improving flow rates of the existing mixing devices could increase the horizontal extent of dispersion, Lake Rotoehu is relatively large (c. 800 ha) compared with other lakes and reservoirs where artificial destratification has been successful, e.g., Weblinger Lake, Germany (17 ha), Blelham Tarn, UK (17 ha), Lake Nieuwe Meer, Netherlands (132 ha), Lake Dalbang, South Korea (529 ha). The lake receives large inputs of solar energy relative to its volume, and modelling suggests that many additional devices would be required to modify mixing in the lake to an extent that would impact water quality on a wider scale.

Nutrient, chlorophyll and water clarity monitoring data reveal promising trends in water quality. It should be noted that Lake Rotoehu stratifies and mixes at time scales of weeks rather than seasonally, hence the predominantly monthly water sampling programme may not characterise all periods of nutrient release and phytoplankton proliferation. Nevertheless, recent trends in Lake Rotoehu of total and inorganic nutrients, particularly phosphorus, are compelling. Total nitrogen and, particularly, total

phosphorus were greatly reduced in 2011-2013 relative to 2009-2011 (TN -16%; TP -31%). Recent seasonal chlorophyll patterns are characterised by maxima during winter, when the water column is usually mixed, rather than during the summer period of frequent stratification events. Winter chlorophyll *a* maxima, usually driven by abundance of diatoms, are typically indicative of healthy lake ecosystem (Ryan et al. 2006). Further, despite strong stratification in summer 2012-13 and 2013-14, major cyanobacterial blooms were not observed.

Phytoplankton community dynamics in Lake Rotoehu followed a pattern commonly observed in eutrophic lakes. Chlorophytes (green algae) and cyanobacteria (blue-green algae) dominated during warmer periods and diatoms dominated community composition when water temperatures were cooler (<15°C) (Wetzel 2001). Changes in phytoplankton relative community abundance appeared to be driven primarily by cyanobacteria total abundance, which was in turn influenced by lake stability. A repeating pattern of high lake stability followed by mixing coincided with increases in cyanobacterial relative and total abundance (Figure 32, Figure 33). At the whole lake scale, the mixing devices had little to no effect on lake stability and therefore did not significantly influence phytoplankton community composition.

Cyanobacteria are able to regulate their buoyancy through the production of gas vesicles, with photosynthetic products (starch) acting as ballast at short (diurnal) time scales (Reynolds and Walsby 1975). This ability can lead to the formation of surface scums and cyanobacteria-dominated communities in lake surface layers (Wetzel 2001). It was expected that these features would be locally disrupted by the vertical mixing produced by the mixing devices in Lake Rotoehu. Cyanobacteria total abundance was observed to be significantly higher in the epilimnion compared to the hypolimnion at the control site (Site 2), but there was no difference in total abundance at the mixing site (Site 1) when the mixing devices were operating (Table 2). This indicates that epilimnion cyanobacterial abundance was higher at Site 2, and the vertical mixing occurring at Site 1 had a homogenising effect on abundance between the epilimnion and hypolimnion, but localised to the area around the mixing device. It should be recognised that the prevailing climate and brief stratification events over the 2012/13 and 2013/14 summers were not conducive to the formation of prolific cyanobacterial blooms. Therefore, extrapolating the disrupting effects of the mixing devices to attenuation of cyanobacterial blooms in the whole lake should be done with caution.

Chlorophyta abundance was homogenous between depths and sites when the mixing devices were not operating, reflecting the prevalence of low lake stability during this time. When the mixing devices were in operation, chlorophyte total abundance was significantly higher in the epilimnion compared to the hypolimnion at the mixing site (Site 1), but not at the control site (Site 2) (Table 2). This difference is primarily related to lower mean abundances of the colonial, non-motile chlorophyte species

*Dictyosphaerium* sp. and *Sphaerocystis* sp. in the Site 1 hypolimnion. These reduced abundances are unlikely to be due to colony disruption during mixing, as colonies appeared intact during enumeration and individual cells would have remained viable (Brown pers. comm.). Similarly, increased turbidity or reduced light availability in the Site 1 hypolimnion can likely be discounted as these species display tolerance to low light levels (Reynolds et al. 2002). The generally low abundance of chlorophyte cells and lack of replicates increases the possibility that the observed difference between the Site 1 epilimnion and hypolimnion is an artificial result, not influenced by the aeration devices. For this reason, the significant differences reported for the cryptophytes (Table 2) should be disregarded.

Zooplankton abundance was dominated by rotifers and copepods, particularly during the summer-autumn period when water temperatures were higher ( $>17^{\circ}\text{C}$ ). Increases in copepod numbers typically coincided with periods of cyanobacterial dominance of the phytoplankton community. This supports the observations by Haney (1987) that calanoid copepods are better suited to cyanobacterial bloom conditions as the New Zealand cladoceran taxa are comparatively depauperate and unsuited to feeding on cyanobacterial colonies (Haney 1987). Some New Zealand calanoid copepod species are known to prey on rotifers, although this appears to be restricted to the larger *Boeckella* species rather than the smaller *Calamoecia* species present in Lake Rotoehu (Couch et al. 1999). The increasing copepod abundance observed during the summer months is more likely related to increasing temperatures and grazing opportunities rather than increasing rotifer abundance.

The timing of peaks in Lake Rotoehu rotifer abundance were similar to those reported by Duggan (1999) for Lakes Tikitapu, Rotoiti, Okaro and Ngaroto for the March 1997 – April 1998 period. These lakes covered a range of trophic status' and thermal stratification characteristics, but all had rotifer peak abundances during the summer-autumn periods (Duggan 1999). Interestingly, the greatest rotifer abundance in Lake Rotoehu in 2011-2014 period was 207 individuals  $\text{L}^{-1}$  (Figure 35). This is markedly less than the peak abundances for Lakes Rotoiti (mesotrophic), Okaro and Ngaroto (eutrophic) (all  $>1000$  individuals  $\text{L}^{-1}$ ) and Tikitapu (oligotrophic) ( $<400$  individuals  $\text{L}^{-1}$ ) (Duggan 1999; Scholes & Bloxham 2008).

Accidental introductions of exotic zooplankton species have been recognised as being detrimental to native plankton communities. For example, Balvert et al. (2009) observed that rotifer abundance declined following the introduction of a more efficient, filter feeding exotic cladoceran species, *Daphnia galeata*, in a newly created lake in the Waikato region. In Lake Rotoehu, *Daphnia galeata* was observed in significant numbers at certain times and it may be competing with native zooplankton species (Duggan et al. 2006; Parkes 2010). However, zooplankton abundance, and in particular cladoceran abundance, is highly variable and difficult to predict, and further research may be

required to determine what effects the introduction of *Daphnia galeata* has on the ecology of Lake Rotoehu. However, an explanation that rotifer numbers were limited by food availability must be considered as equally plausible (Duggan 1999). The declining trophic level of Lake Rotoehu for the 2011-14 period (Figure 1) was associated with lower than expected phytoplankton abundance for a eutrophic lake (Brown pers. comm.) and this is likely to be a contributing factor for lower comparative zooplankton abundance.

Rotifer abundance was significantly lower in the control site (Site 2) hypolimnion compared to the mixing site (Site 1) hypolimnion when the mixing devices were switched off. Lower numbers of rotifers were also observed in the epilimnion of Site 2 compared to Site 1 but the t-test was marginal ( $P=0.06$ ) with regard to this difference being significant (Table 3). This suggests that rotifer abundance was not uniformly distributed across the lake, especially during the first 12 months of sampling. This may be related to the lower lake stability at this time causing patchiness in resources or due to internal wave dynamics from increased wind causing aggregations. In contrast, when the mixing devices were operating there was no significant difference in total rotifer numbers between sites and depths. However, comparisons of individual species abundance between depths at each site suggest that some homogenisation of rotifer abundance may have occurred at Site 1 compared to Site 2, but this pattern was generally overwhelmed by natural variation.

The observed significant differences (t-test;  $P<0.001$ ) in cladoceran abundances between the epilimnion and hypolimnion of both Site 1 and Site 2 when the mixing devices were operating (Table 3) should be treated with caution. Zooplankton community distributions are known to be partially resistant to vertical mixing and are structured not only by physical, but also biological processes (Folt & Burns 1999). Given that cladoceran abundances were generally low during mixing device operation and often peaked during periods when the mixing devices were not operating, attempting to attribute an effect on cladoceran populations from the mixing devices is not justified.

Bray-Curtis similarity between sites and depths predominantly ranged from 60-85% (Figure 37; Figure 38). A single departure from this pattern occurred between the mixing site (Site 1) epilimnion and hypolimnion in February 2014 when Bray-Curtis similarity decreased to 44.4%; in comparison the difference between Site 2 (control site) epilimnion and hypolimnion remained similar at 70.9%. This result is counter to the expected homogenisation of the plankton community at Site 1 when the mixing devices were operating. In addition, there was no large deviation in similarity between Site 1 and Site 2 for either depth at that time. Closer examination of the community structure revealed an increased proportion of minor phytoplankton species (e.g. *Closterium* sp., *Coelastrum* sp., *Scenedesmus* sp., *Sphaerocystis* sp., *Synedra* sp.) in the Site 1 hypolimnion that were not present in the epilimnion. The low abundances of these

species ( $<100$  cells  $\text{mL}^{-1}$ ) mean they are likely to be of little ecological significance and the transient drop in Bray-Curtis similarity is not indicative of a major effect on the local plankton community. This was confirmed by analysis of the phytoplankton and zooplankton communities as Bray-Curtis similarity for the phytoplankton community was comparable in degree and pattern to that observed for the combined plankton community. Zooplankton community Bray-Curtis similarity was also analogous to that of the combined community, apart from a single occurrence in the Site 1 epilimnion on 31 January 2013 when zooplankton abundance was comparatively low. This decline in similarity between sites and depth does occur during a period when the mixing devices were operating, but the effect was not sustained and is therefore difficult to attribute to the devices alone. Similarly, neither the prevailing meteorological conditions nor the lake stability were remarkable at the time. Without finer scale sampling of the zooplankton community during this period it is not possible to provide a definite explanation for the change in the zooplankton community.

Although increased water column mixing has the potential to reduce the severity and aesthetic impact of cyanobacteria blooms, the results highlight the importance of managing nutrients to control the occurrence of algae blooms in Lake Rotoehu. Specifically, the observed restriction of the supply of inorganic phosphorus during stratified periods over the most recent summers coincides with reduced summer phytoplankton concentrations. Although N-fixing cyanobacteria are capable of meeting shortfalls in nitrogen supply, phosphorus supply cannot be circumvented (Reynolds et al. 2002). Further work could be aimed at quantifying the drivers of the observed reduction in nutrients, i.e. the relative contributions of atmospheric contributions, land management, and the action of P-binding in inflows and/or sediments via inflow dosing with alum. These aspects are likely to have important implications for the management of Lake Rotoehu.

## Conclusions

Monitoring data have shown that the present artificial mixing devices are capable of affecting water column thermal structure locally, on a scale of tens to at most a few hundred metres. Although refinement of these installations could improve their performance, it is likely that the existing machines are incapable of effecting significant thermal change on a basin-wide scale. This conclusion has been corroborated both by monitoring over recent years, and by ecosystem modelling. Deployment of mixing devices in Rotoehu has provided a valuable indication of the scale of application required to effectively mix medium to large-sized lakes.

Large inter-annual and seasonal variations in plankton abundance and diversity have confounded attempts to isolate the effects of the mixing devices at the species level.

Some encouraging results with regard to cyanobacteria distribution have been observed at the local scale, but these need to be placed into the context that abundances were generally lower than in previous years, particularly in the 2000s. The effects of the mixing devices on zooplankton populations were difficult to determine due to confounding factors such as the presence of an invasive species and low phytoplankton abundance. Published reports generally conclude that artificial mixing has little direct effect on zooplankton communities but does affect the composition of phytoplankton communities which in turn influences zooplankton community composition.

A further summer deployment with monitoring could help to optimise the performance of the mixing devices, and better quantify their capability to contribute to water quality improvements in Lake Rotoehu. Increased frequency of discharge measurements from the mixing devices would also assist with future monitoring programmes.

## References

- Abell JM, Özkundakci D & Hamilton DP (2010). Nitrogen and phosphorus limitation of phytoplankton growth in New Zealand lakes: implications for eutrophication control. *Ecosystems* 13: 966-977.
- Ashley KI (1983a). Hypolimnetic aeration of a naturally eutrophic lake: physical and chemical effects. *Canadian Journal of Fisheries and Aquatic Sciences* 40: 1343-1359.
- Ashley KI (1983b). Hypolimnetic aeration and functional components of the lake ecosystem: phytoplankton and zooplankton effects. In: *Lake Restoration, Protection and Management*. Taggart, J and Moore, L (Eds). Proc. Second Annual Conference of the North American Lake Managers Society 2: 31-40).
- Chapman MA, Green JD & Jolly VH (1985). Relationships between zooplankton abundance and trophic state in seven New Zealand lakes. *Hydrobiologia* 123: 119-136.
- Chapman, MA & Lewis MH (1976). *An Introduction to the Freshwater Crustacea of New Zealand*. Collins, Auckland: 261 pp.
- Couch KM, Burns CW & Gilbert JJ (1999). Contribution of rotifers to the diet and fitness of *Boeckella* (Copepoda: Calanoida). *Freshwater Biology* 41: 107-118.
- Donovan CL (2003). Estimate of the Geothermal Nutrient Inputs to Twelve Rotorua Lakes. Bioresarches Group Limited, prepared for Environment Bay of Plenty.
- Dake JM & Harleman DR (1969). Thermal stratification in lakes: analytical and laboratory studies. *Water Resources Research* 5: 484-495.
- Duggan IC (1999). The Distribution and Dynamics of Planktonic Rotifera in the North Island, New Zealand. Unpublished PhD Thesis. University of Waikato. Hamilton p246.
- Duggan IC, Green JD & Burger DF (2006). First New Zealand records of three non-indigenous Zooplankton species: *Skistodiaptomus pallidus*, *Sinodiaptomus valkanovi*, and *Daphnia dentifera*. *New Zealand Journal of Marine and Freshwater Research* 40: 561-569.
- Environment Bay of Plenty, Rotorua District Council and Te Arawa Maori Trust Board (2007). *Lake Rotoehu Action Plan*. (Vol. 9372).
- Folt CL & Burns CW (1999). Biological drivers of zooplankton patchiness. *Trends in Ecology & Evolution* 14: 300-305.
- Haney F (1987). Field studies on zooplankton-cyanobacteria interactions, New Zealand. *Journal of Marine and Freshwater Research* 21: 467-475.
- Heo WM & Kim B (2004). The effect of artificial destratification on phytoplankton in a reservoir. *Hydrobiologia* 524: 229-239.
- Hötzel G & Croome R (1999). *A Phytoplankton Method Manual for Australian Freshwaters*. Land and Water Resources Research and Development Corporation Occasional Paper 22/99, Canberra, Australia.

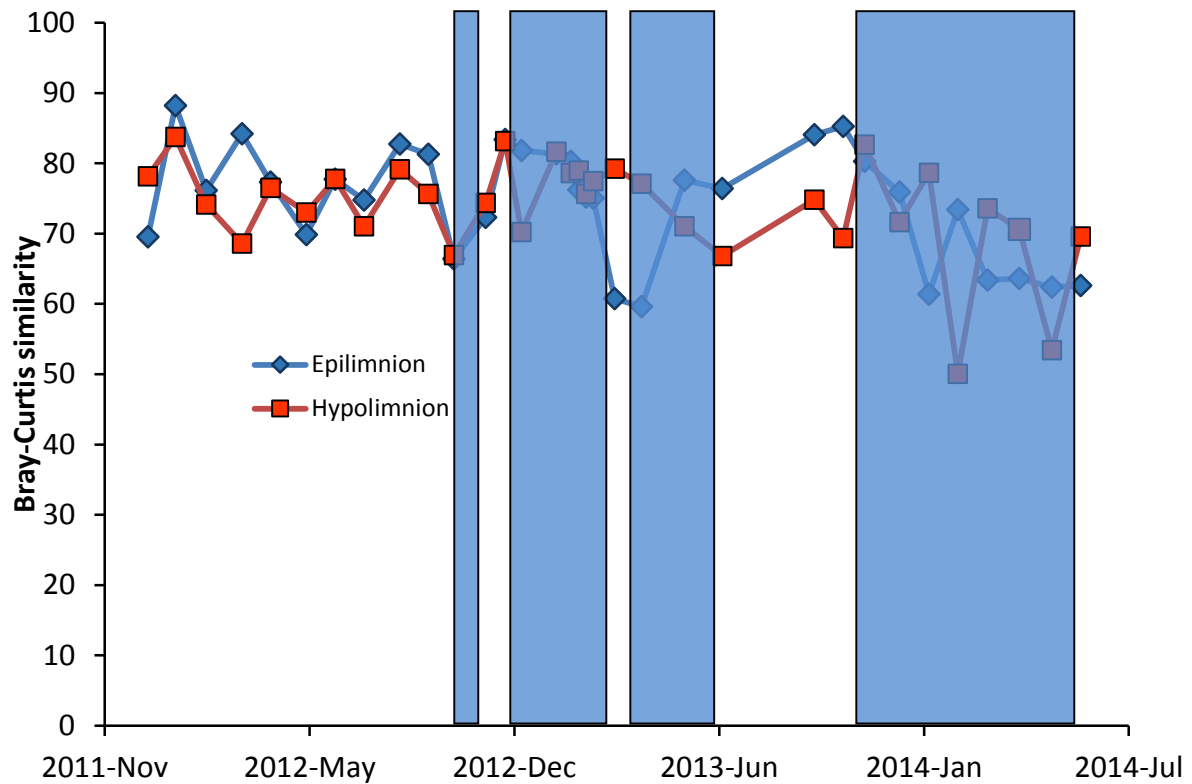


- Jeppesen E, Lauridsen T, Mitchell SF & Burns CW (1997). Do planktivorous fish structure the zooplankton communities in New Zealand lakes? *New Zealand Journal of Marine and Freshwater Research* 31: 163-173.
- Jeppesen E, Søndergaard M, Jensen JP, Havens KE, Anneville O, Carvalho L. ... & Winder, M. (2005). Lake responses to reduced nutrient loading—an analysis of contemporary long-term data from 35 case studies. *Freshwater Biology* 50: 1747-1771.
- Lackey RT (1973). Effects of artificial destratification on zooplankton in Parvin Lake, Colorado. *Transactions of the American Fisheries Society* 102: 450-452.
- Leech DM & Williamson CE (2000). Is tolerance to UV radiation in zooplankton related to body size, taxon, or lake transparency? *Ecological Applications* 10: 1530-1540.
- Lund J WG (1971). An artificial alteration of the seasonal cycle of the plankton diatom *Melosira italica* susp. *subarctica* in an English lake. *Journal of Ecology* 59: 521-533.
- McClintock NL & Wilhm J (1977). Effects of artificial destratification on zooplankton of two Oklahoma reservoirs. *Hydrobiologia* 54: 233-239.
- McLaren IA (1963). Effects of temperature on growth of zooplankton, and the adaptive value of vertical migration. *Journal of the Fisheries Board of Canada* 20: 685-727.
- Miles NG & West RJ (2011). The use of an aeration system to prevent thermal stratification of a freshwater impoundment and its effect on downstream fish assemblages. *Journal of fish Biology* 78: 945–52.
- Oliver RL, Hamilton DP, Brookes JD & Ganf GG (2012). Physiology, blooms and prediction of planktonic cyanobacteria. Chapter 6. In: *Ecology of Cyanobacteria II: Their Diversity in Space and Time*. Whitton, BA (Ed). Springer. Netherlands
- Parkes SM (2010) *Constructed Waters Facilitated by Simple Communities*. Unpublished MSc Thesis. University of Waikato. Hamilton. p119.
- Ptacinik R, Diehl S, & Berger S (2003). Performance of sinking and nonsinking phytoplankton taxa in a gradient of mixing depths. *Limnology and Oceanography* 48: 1903-1912.
- Read JS, Hamilton DP, Jones ID, Muraoka K, Winslow LA, Kroiss R, Wu CH & Gaiser E (2011). Derivation of lake mixing and stratification indices from high-resolution lake buoy data. *Environmental Modelling and Software* 26: 1325-1336.
- Reynolds C S & Walsby AE (1975) Water-blooms. *Biological Reviews* 50: 437-481.
- Ryan EF, Duggan IC, Hamilton DP, & Burger DF (2006). Phytoplankton assemblages in North Island lakes in New Zealand: is trophic state, mixing, or light climate more important? *New Zealand Journal of Marine and Freshwater Research* 40: 389–398.
- Scholes P (2009). Rotorua Lakes Water Quality Report 2009. Environmental Publication 2009/12. Environment Bay of Plenty. Whakatane. p92.

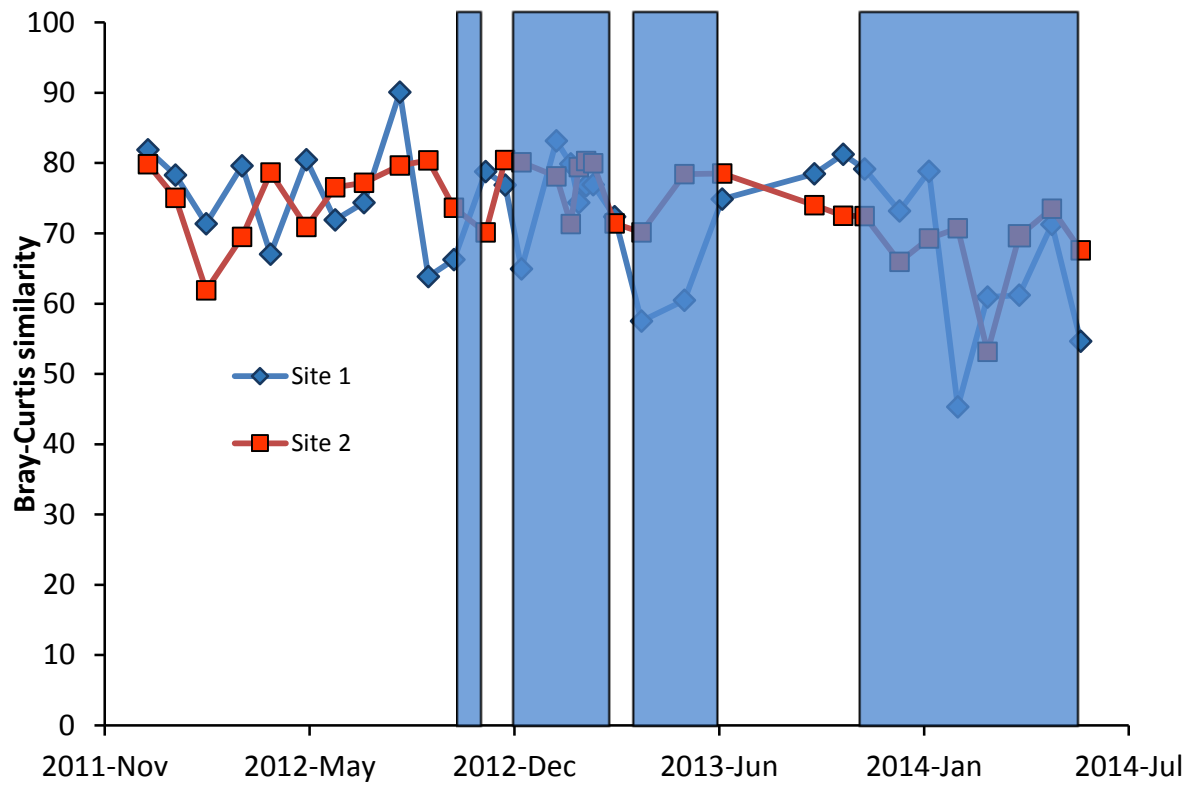


- Scholes P & Bloxham M (2008). Rotorua Lakes Water Quality Report 2007. Environment Bay of Plenty. Rotorua, New Zealand.
- Shiel RJ (1995). A Guide to the Identification Of Rotifers, Cladocerans and Copepods from Australian Inland Waters. Co-operative Research Centre for Freshwater Ecology, Murray-Darling Freshwater Research Centre. Albury, NSW. 144 pp.
- Søndergaard M, Jensen JP & Jeppesen E (2003). Role of sediment and internal loading of phosphorus in shallow lakes. *Hydrobiologia* 506: 135-145.
- Toffolon M & Serafini M (2013). Effects of artificial hypolimnetic oxygenation in a shallow lake. Part 2: numerical modelling. *Journal of Environmental Management* 114: 530–9.
- Trolle D, Hamilton DP, Pilditch CA, Duggan IC & Jeppesen E (2011). Predicting the effects of climate change on trophic status of three morphologically varying lakes: Implications for lake restoration and management. *Environmental Modelling and Software* 26: 354-370.
- US Environmental Protection Agency 2007. Standard Operating Procedure for Phytoplankton Analysis. US Environmental Protection Agency: 42 pp.
- Utermöhl H (1958). Zur Vervollkommung der quantitativen phytoplankton-methodik. *Mitteilungen Internationale Vereinigung für Theoretische und Angewandte Limnologie* 9:38.
- Wetzel RG. *Limnology: Lake and River Ecosystems*. 3rd Edition. Academic Press. San Diego, p1006.
- Wilcock RJ, Monaghan RM, Quinn JM, Campbell AM, Thorrold BS, Duncan MJ, McGown AW & Betteridge K (2006). Land-use impacts and water quality targets in the intensive dairying catchment of the Toenepi Stream, New Zealand. *New Zealand Journal of Marine and Freshwater Research* 40: 123-140.

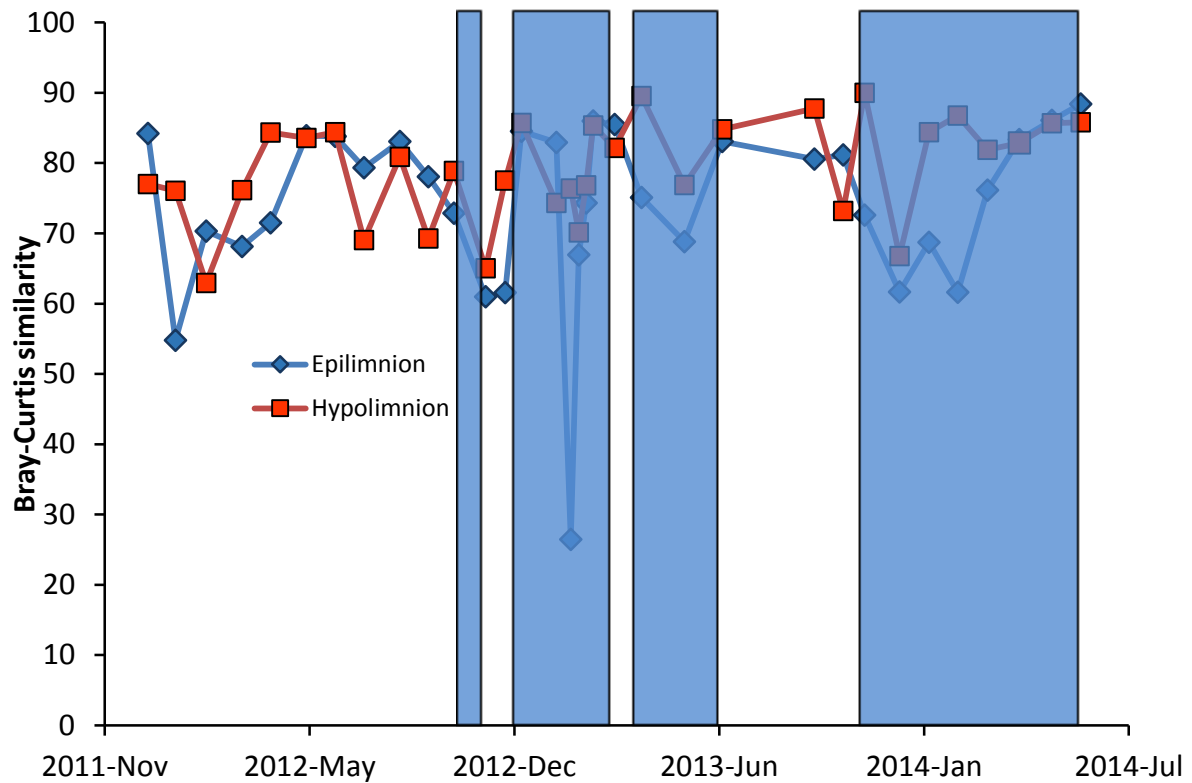
## Appendix 1

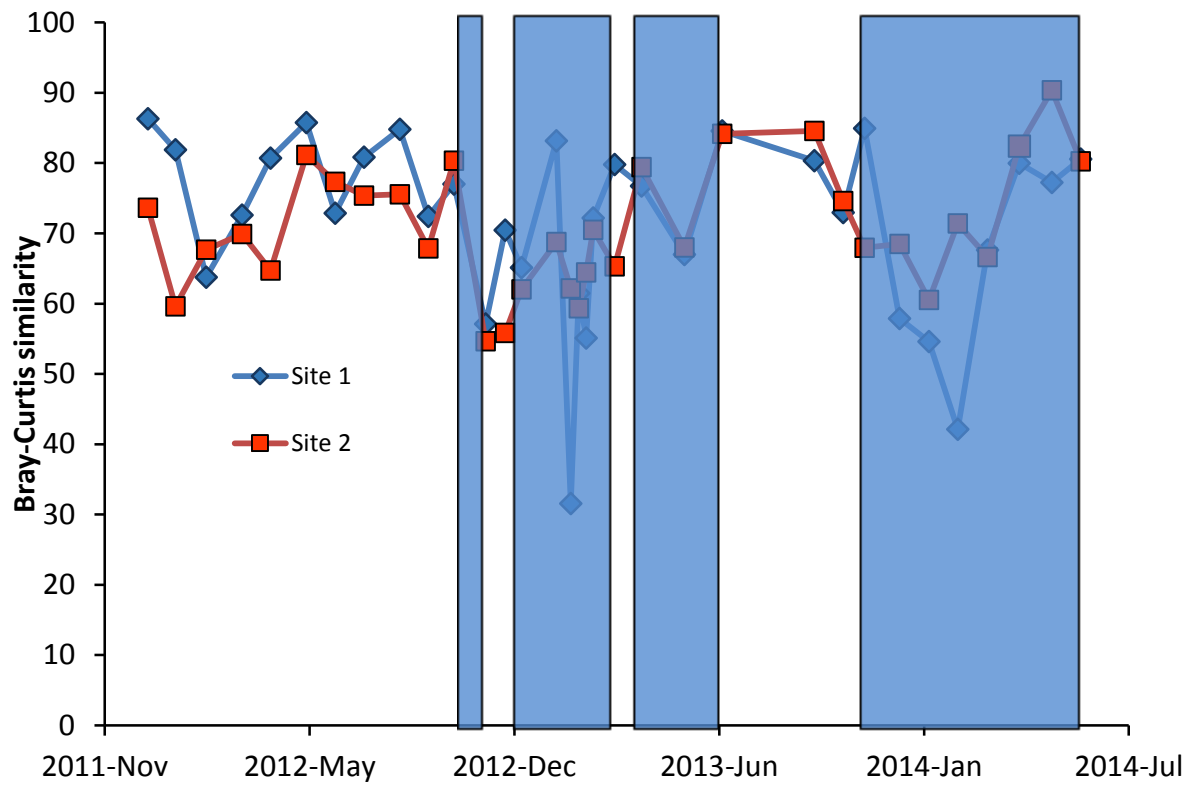


Appendix 1.1. Degree of similarity (Bray-Curtis) in phytoplankton community composition between Site 1 (mixing) and Site 2 (Control) for both the epilimnion (0.5 m) and hypolimnion (9 m) layers in Lake Rotoehu between 16 December 2011 and 13 June 2014. Shaded sections indicate periods when mixing devices were in operation.



Appendix 1.2. Degree of similarity (Bray-Curtis) in phytoplankton community composition between the epilimnion (0.5 m) and hypolimnion (9 m) layers of the Site 1 (mixing) and Site 2 (Control) locations in Lake Rotoehu between 16 December 2011 and 13 June 2014. Shaded sections indicate periods when mixing devices were in operation.





Appendix 1.4. Degree of similarity (Bray-Curtis) in zooplankton community composition between the epilimnion (0.5 m) and hypolimnion (9 m) layers of the Site 1 (mixing) and Site 2 (Control) locations in Lake Rotoehu between 16 December 2011 and 13 June 2014. Shaded sections indicate periods when mixing devices were in operation.

Appendix 1.5. Sampling dates for nutrient concentrations, chlorophyll *a* concentrations, zooplankton and phytoplankton and CTD casts. Note dye tracer and ADCP study was conducted on 27 and 28 February 2013.

Sampling dates	Comments
15/12/2011	Sampling commences
11/01/2012	
10/02/2012	
16/03/2012	
13/04/2012	
18/05/2012	
15/06/2012	
13/07/2012	Mixing devices installed
17/08/2012	
14/09/2012	
9/10/2012	
9/11/2012	
28/11/2012	
14/12/2012	
17/01/2013	Intensive sampling period
31/01/2013	
8/02/2013	
15/02/2013	
22/02/2013	
15/03/2013	
10/04/2013	
22/05/2013	Devices switched off & sampling halted
28/06/2013	
26/09/2013	
24/10/2013	
14/11/2013	
18/12/2013	
16/01/2014	
13/02/2014	Devices restarted
14/03/2014	
14/04/2014	
16/05/2014	
13/06/2014	
	Devices switched off end June